

UNCLASSIFIED

AD 4 3 8 2 3 3

DEFENSE DOCUMENTATION CENTER

FOR

SCIENTIFIC AND TECHNICAL INFORMATION

CAMERON STATION, ALEXANDRIA, VIRGINIA



UNCLASSIFIED

NOTICE: When government or other drawings, specifications or other data are used for any purpose other than in connection with a definitely related government procurement operation, the U. S. Government thereby incurs no responsibility, nor any obligation whatsoever; and the fact that the Government may have formulated, furnished, or in any way supplied the said drawings, specifications, or other data is not to be regarded by implication or otherwise as in any manner licensing the holder or any other person or corporation, or conveying any rights or permission to manufacture, use or sell any patented invention that may in any way be related thereto.

64-13

438233

DDC

DOWNEY PLANT

RESEARCH AND ENGINEERING DIVISION

PARTICLE-SIZE DETERMINATION OF AEROSOLS BY THE PHOTOEXTINCTION TECHNIQUE

Investigation Under

U. S. Army Chemical Center
Contract DA-18-108-405-CML-829

Special Report No. 0395-04(17)SP/February 1964/Copy 1

438233

DDC
MAY 8 1964



AEROJET-GENERAL CORPORATION
Research and Engineering Division
11711 Woodruff Avenue
Downey, California

PARTICLE-SIZE DETERMINATION OF AEROSOLS BY
THE PHOTOEXTINCTION TECHNIQUE

by

R. L. MacLean

Special Report No. 0395-04(17)SP

Investigation Under

U.S. Army Chemical Center
Contract DA-18-108-405-CML-829

Reviewed by: R. B. Mortensen
R. B. Mortensen, Head
Terminal Ballistics Dept
Research Division

Date: 6 March 1964

No. of Pages: 63

Approved by: H. J. Fisher
H. J. Fisher, Manager
Research Division

Classification: UNCLASSIFIED

ABSTRACT

A photoextinction method has been developed to determine particle-size distributions of settling aerosols in a large test chamber. The theory of photoextinction by aerosol particles was explored and applied to a method of determining particle-size distributions from decay measurements based on Stokes' law.

A photometric measuring apparatus was constructed and installed in the testing facility. Measurements of changes in light transmission were made for several dissemination experiments. Data reduction procedures were investigated with the data obtained. Errors in both theory and measuring instrumental parameters are discussed.

Methods to determine particle-size distributions and additional studies of the photoextinction technique are recommended.

CONTENTS

	<u>Page No.</u>
1. INTRODUCTION	1
2. THEORY	2
2.1 Light Extinction	2
2.2 Sedimentation	8
3. INSTRUMENTATION	17
3.1 General Description	17
3.2 Lens System	17
3.3 Calibration	24
3.4 Instrumentation Limitations	25
4. DATA REDUCTION	30
5. ERROR EVALUATION	32
6. EXPERIMENTAL RESULTS	34
6.1 GS Series	34
6.2 DB Series	36
6.3 PX Series	36
6.4 FP Series	43
7. CONCLUSIONS	54
8. RECOMMENDATIONS	55
REFERENCES	56

ILLUSTRATIONS

<u>Figure No.</u>		<u>Page No.</u>
1.	Rose's Extinction Coefficient vs Particle Size	4
2.	Maximum Particle Diameter vs Reynolds' Number	10
3.	Deviation of Drag Coefficient From Stoke's Law	12
4.	Photoextinction System Composite	18
5.	Photoextinction Device Receiver	19
6.	Photoextinction Device - Light Source	20
7.	Projector and Window Assembly	21
8.	Telescope Detector Assembly	22
9.	Photoelectric Controller	23
10.	Typical Calibration Curves From Photoextinction Measurements	26
11.	Mass Effect for Silica on Photoextinction Size Distribution Curves	35
12.	Transmission Curves for DB Series	37
13.	Size Distribution for Salt by Photoextinction, Harner and Musgrave Method (a)	38
14.	Size Distribution for Salt by Photoextinction, Harner and Musgrave Method (b)	39
15.	Size Distribution for Salt by Photoextinction, Harner and Musgrave Method (c)	40
16.	Size Distribution for Salt by Photoextinction, Harner and Musgrave Method (d)	41

ILLUSTRATIONS (Cont)

<u>Figure No.</u>		<u>Page No.</u>
17.	Average Size Distribution Curves for DB Salt Series, Photoextinction, Harner and Musgrave Method	42
18.	Size Distributions of Bis-Uvinul Solutions by Hot-Gas Dissemination, Harner and Musgrave Method, Condition 1	44
19.	Size Distributions of Bis-Uvinul Solutions by Hot-Gas Dissemination, Harner and Musgrave Method, Condition 2	45
20.	Size Distributions of Bis-Uvinul Solutions by Hot-Gas Dissemination, Harner and Musgrave Method, Condition 3	46
21.	Size Distribution Curves for Silica From Photoextinction, Harner and Musgrave Method	47
22.	Data Reduction Comparison of two Methods - Still Settling, (1) Harner and Musgrave, and (2) Michaels-Millipore.	48
23.	Data Reduction Comparison of two Methods - Stirred Settling, (1) Harner and Musgrave, and (2) Michaels-Millipore.	49
24.	Size-Distribution Curves for Silicone-Coated Silica, Harner and Musgrave Method	51
25.	Size-Distribution Curves for Silicone- Coated Silica, Michaels-Millipore Method.	52
26.	Average Distribution Curves From Photoextinction and Millipore Filters	53

1. INTRODUCTION

This report summarizes the theory and experimental results from an evaluation of a photoextinction method for measuring particle-size distributions in aerosols. It is submitted in partial fulfillment of Contract DA-18-108-CML-829. In searching for accurate and reproducible methods for measuring and controlling particle size, nearly every physical and chemical approach was investigated by many workers and many instruments were developed. It has become evident that no technique or instrument can be equally successful in measuring all materials or particle-size ranges. Each should be considered as a separate problem requiring specific techniques.

Many techniques have been utilized for measuring and defining particles in terms of size distribution relations. Principles that have been employed in particle-size assessment include sedimentation, sieving, microscopy, permeametry, absorption, light scattering, change in electrolytic resistivity, flow impaction, X-ray, sonic vibrations, bulk density and rate of packing, magnetochemistry, and precipitation of charged particles. All these methods have specific theoretical and experimental limitations and must be carefully evaluated. When the information desired is to describe an aerosol in terms of its effective size distribution during decay, the effects the experimental measurements have on the data should be considered. Generally, when an aerosol sample is taken, the method of sampling or handling will significantly alter the size properties. Photoextinction measurements of a decaying cloud appear to offer considerable advantages for aerosols within specific limits. The light beam used does not introduce significant additional energy into the system observed; readings can be made any time; and the light beam effectively samples a diameter of the cloud instead of a point within the cloud. The measurements are made continuously as the aerosol is settling which facilitates the collection of more complete data compared to methods requiring periodic physical sampling with subsequent analysis. Photoextinction is well described in literature along with the sedimentation theory employed in this technique. There are numerous sources of possible errors in applying the theory. There are also limitations in experimental techniques. However, it is felt that corrections may be made mathematically or by standardizing the system to achieve meaningful size-distribution information. Considering the advantages of photometric measurements on the original aerosol, this technique was chosen for evaluation in Aerojet's large test chamber.

2. THEORY

The photoextinction technique is principally a method for measuring the change in light absorbed by particles dispersed in a medium as the particles settle. The apparatus consists of a beam of approximately parallel light projected across the suspension onto a photoelectric cell. The beam diameter is small compared to the distance of the beam below the surface of the suspension. Measurements of the emergent light intensity are recorded at time intervals (or continuously) while the particles settle out of the suspension under the influence of gravity.

2.1 LIGHT EXTINCTION

Particles that are small compared to the wavelength of light have an absorbancy in accordance with Rayleigh's law. Rayleigh's law states that the intensity of scattered light varies directly as a function of particle radius to the sixth power and inversely as the fourth power of the wavelength of light. The size below which such transmission begins is given as about 0.1μ by Dallavalle (Reference 1), 0.5μ by Schweyer and Work (Reference 2), 0.6μ by Stutz (Reference 3), and 2.0μ by Richardson (References 4 and 5). According to Skinner and Withes (Reference 6), the variation of these values depends upon the optical geometry of the instrument used. The relation which governs the transmission through a suspension of monodisperse particles in this size region may be described (Reference 7) by the expression:

$$I = I_0 \exp \left(-k n \frac{V^2}{\lambda^4} \right) \quad (1)$$

where

I, I_0 = transmitted and incident light intensities

k = constant involving refractive indices

n = number of particles per unit volume of the suspending media

V = volume per particle

λ = wavelength of light used.

This relation shows that longer wavelengths will be transmitted more freely and the total absorbancy will decrease rapidly as the particle diameter approaches 0. The strong inverse dependence of the transmission on particle diameter in this region has been confirmed by other workers (References 1, 7, and 8).

For particles much larger than the wavelength of light, transmission is generally considered to follow the "square law" of geometrical optics in which the light blocked is proportional to the projected cross-sectional area of the suspension of particles. For particles greater than 1μ dia, the transmission has been shown to be independent of wavelength, (References 2, 3, 9, and 10).

The transmission behavior of particles from near 0 dia up to relatively large sizes has been studied by Rose (Reference 8). The extinction was measured for a group of different size powders and compared with the theoretical values. Figure 1 shows the results presented by Rose as a relation between particle size and extinction coefficient. The extinction coefficient is defined as the actual blocking power of a particle divided by the theoretical blocking power according to the "square law" of geometric optics.

The expression for the transmission of light through a uniform suspension of particles generally used (Reference 2) is a form of the Lambert-Beer law written as:

$$\ln \frac{I_0}{I} = A c l \quad (2)$$

where

I, I_0 = transmitted and incident light intensities

A = projected area/gram of particles in the light beam
(includes all of the optical factors involved)

c = concentration of particles per unit volume

l = length of light path

In this expression, Ac is the projected area per unit volume. Therefore the plot of the ratio $(\ln I_0/I_t) / (\ln I_0/I)$ vs the values of particle size as computed from Stokes' equation for time, t , gives the cumulative distribution by area, where I_t is the intensity of transmitted light at time t , and I is the intensity in the original homogeneous suspension at time 0.

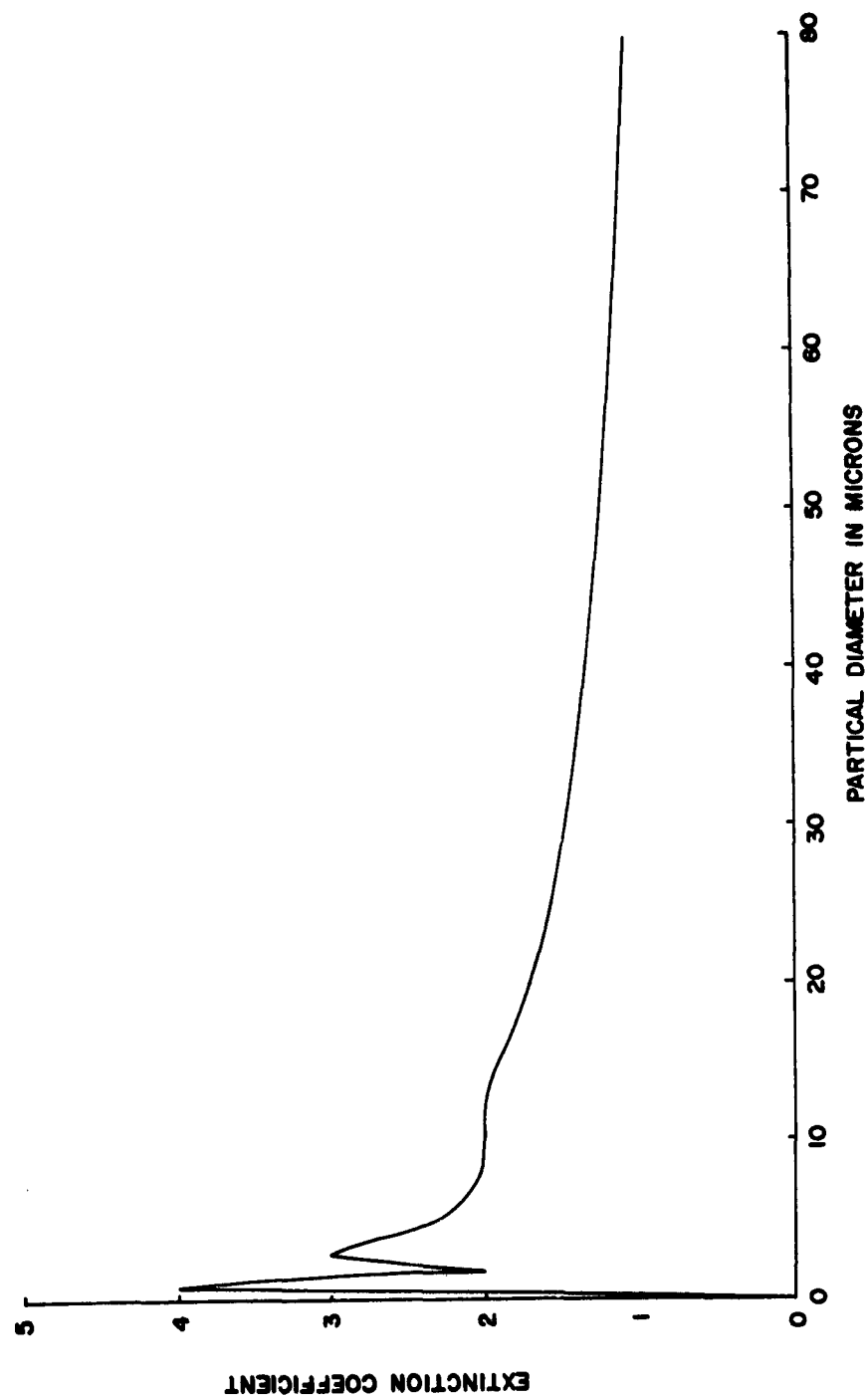


Figure 1. Rose's Extinction Coefficient vs Particle Size.

In most aerosols however, the particles are not uniform, but contain a distribution of sizes. A more complete description, applicable to a nonuniform distribution is given by Rose (Reference 8) as:

$$\ln \frac{I_0}{I} = Kcl \sum_0^d K_x n_x d_x^2 \quad (3)$$

where

I_0, I = incident and transmitted light intensities

K = constant

c = concentration of particles in light beam, g/cc

l = length of light path, cm

K_x = Rose's extinction coefficient, which equals the ratio of the actual obscuring power of a particle of diameter d_x theoretically according to the square law of geometrical optics.

n_x = number of particles of diameter d_x per g of powder

d_x = maximum size particle in suspension, cm

From Equation 3 it is clear that for specific particle diameters d_1 and d_2 :

$$\begin{aligned} Kcl \sum_{d_1}^{d_2} K_x n_x d_x^2 &= Kcl \sum_0^{d_2} K_x n_x d_x^2 - Kcl \sum_0^{d_1} K_x n_x d_x^2 \\ &= \ln \frac{I_0}{I_2} - \ln \frac{I_0}{I_1} \end{aligned} \quad (4)$$

then

$$Kcl \sum_{d_1}^{d_2} K_x n_x d_x^2 = \ln \frac{I_0}{I_2} - \ln \frac{I_0}{I_1} \quad (5)$$

where I_1 and I_2 are the transmitted light intensities through suspension of particles ranging from 0 to d_1 and 0 to d_2 respectively and $I_1 > I_2$.

For small intervals:

$$K_{cl} n_x d_m^2 = \frac{I_1 - I_2}{K_m} \quad (6)$$

where

d_m = mean diameter of interval d_1 to d_2

K_m = Rose's extinction coefficient for d_m

Since $K_{cl} n_x d_m^2$ represents the actual total cross-sectional area of particles in the given interval, per unit area of beam, then multiplying by d_m and a proportionality constant C , gives the value for the total particle volume of increment d_1 to d_2 .

$$C (K_{cl} n_x d_m^2) d_m = C \frac{d_m}{K_m} (I_1 - I_2) \quad (7)$$

= total particle volume per unit
area of beam

Knowing the density of the particle, a mass relation may be calculated. Applying this relation for all the intervals in the settling of a suspension, a mass-size distribution can be determined. The fraction of the mass F_i , found in the i th particle-size interval is computed using the following expression:

$$F_i = \frac{\left(\frac{d_i}{K_x} \right) \left(\frac{I_o}{I_{i+}} - \frac{I_o}{I_{i-}} \right)}{\sum_{i=0}^n \left(\frac{d_i}{K_x} \right) \left(\frac{I_o}{I_{i+}} - \frac{I_o}{I_{i-}} \right)} = \frac{\left(\frac{d_i}{K_x} \right) \sum_{d_{i-}}^{d_{i+}} K_x N d^2}{\sum_{i=0}^n \left(\frac{d_i}{K_x} \right) \sum_{d_{i-}}^{d_{i+}} K_x N_x d^2} \quad (8)$$

where

n = the number of size intervals

N = the number of particles per cc of diameter d in light beams

d_i = the midpoint diameter of the particle-size intervals

The derivation of these equations depends on several assumptions:

- a. The particles are absolutely opaque.
- b. There is no reflection between particles or between particles and the walls of the chamber.
- c. Any deviations in the light obscuring power of a small particle from that given by the square law is covered by the factor K_x ; which should thus depend on the particle size, wavelength of light, refractive index of particle and fluid, etc., but not upon the physical size of the apparatus.
- d. The concentration of the suspension is such that no two particles, within the suspension, fall on the same line parallel to the light beam.

Detailed discussions of the effects of the foregoing assumptions are given in References 8, 11, 12, 13, and 14. Other sources of error are inherent in the instrument used for the measurements. It was concluded that a transparent particle behaves as though it is opaque, provided that there is sufficient difference between the refractive index of the settling medium and the particle, and also that the monitored area of the light beam subtends a sufficiently small solid angle at the center of the suspension. Rose recommends the subtended angle be a maximum of 1° (or 0.00024 solid radians). Limiting the subtended angle which reduces effects of forward scattering to a minimum is also a condition for eliminating errors arising from the transparency of the particles. The adoption of Rose's extinction coefficient, K_x , should serve as an acceptable relation of light obscured to actual particle-size cross-sections. The effect of particles hiding behind each other in the light beam can be calculated statistically and the concentration of particles may be controlled within the desired limits.

Because of the many sources of error in both adherence of theory and experimental limitations, the photoextinction method is seldom used for absolute measurements. However, because of its convenience in application and sampling advantages, it is an excellent method for routine comparisons of powdered materials.

2.2 SEDIMENTATION

Sedimentation principles have been used extensively in methods for particle-size determination.

2.2.1 Tranquil Settling

The photoextinction techniques as well as others, depend on the relation of settling velocities to specific particle sizes. The rate of fall (u) of a spherical particle is related to the diameter of the particle (d) by Stokes' law in the form of:

$$d = \frac{18 \eta u}{(\rho_1 - \rho_2) G} \quad (9)$$

where

G = gravitational constant

ρ_1 = density of particle

ρ_2 = density of suspension medium

η = viscosity of medium

u = settling velocity of particle

This expression may be rewritten as:

$$t = \frac{18 \eta h}{d^2 (\rho_1 - \rho_2) G} \quad (10)$$

where

t = time required for a given particle size, d , to fall a given height, h

h = height of fall from top surface of suspension at time 0 to light beam

This relation is almost always used to convert results of sedimentation tests into particle-size distributions. The application of this equation has a number of limitations which should be considered.

Stokes' law is valid only when the resistance to the motion of the particle is almost entirely due to the viscosity of the suspending medium. The inertia of the medium should have little effect. Flow of the medium past a particle is almost entirely viscous if the particle is small enough. However, with increasing particle size, a wake begins to develop behind the particle and inertial effects assume an increasing importance. The Reynolds' number indicates the ratio of inertial forces to the viscous forces. The Reynolds' number is a dimensionless quantity, which, for spherical particles falling through a fluid, is defined as ud/v , where u is the velocity of fall through the medium (terminal velocity), d is the diameter of the sphere, and v is the kinematic viscosity of the medium. The kinematic viscosity is the absolute viscosity divided by the density of the medium. Davies (Reference 15) has estimated that the Reynolds' numbers corresponding to errors of 1, 5, and 10% in the velocities of settling particles are 0.074, 0.38, and 0.82 respectively. From Equation 10 and the definition of Reynolds' number, the following equation can be obtained relating the maximum particle size d_c , to which Stokes' law applies to the maximum Reynolds' number, Re_c :

$$d_c^3 = \frac{18 Re_c \eta^2}{\rho_2 (\rho_1 - \rho_2) G} \quad (11)$$

The maximum particle size calculated for a Reynolds' number of 0.5 for silica (density 2.5) in air is 46.5 μ . Particles with a density of 1.0 would have a maximum particle size of 63 μ . Figure 2 indicates the maximum particle sizes for different Reynolds' numbers and particle densities.

Stokes' law may be expressed in a form using drag functions as in Reference 16.

$$D_t = 3 \eta u \pi d = C_D \frac{\rho u^2}{2} \pi \frac{d^2}{4} \quad (12)$$

where

D_t = total drag

C_D = drag coefficient

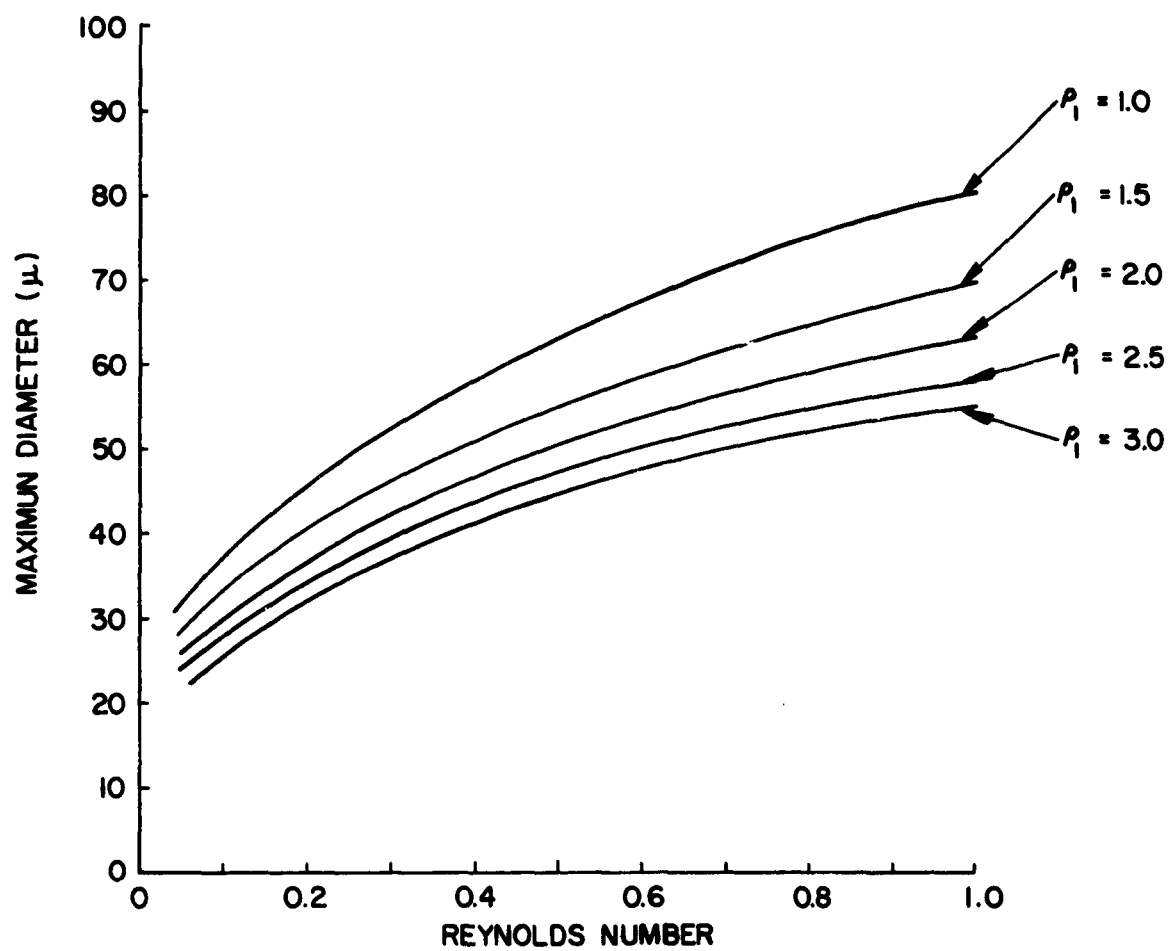


Figure 2. Maximum Particle Diameter vs Reynolds' Number.

Experiments show that for Reynolds' numbers below 0.4 in a sphere, the drag coefficient C_D is a constant following the relation $C_D = 24/Re$. Figure 3 shows a plot of the variation of drag coefficient from Stokes' law with Reynolds' number. It can be seen that for Reynolds' numbers of 0.5 or less the deviation from Stokes' law is within 6%. Based on this approximation, a Reynolds' number of 0.5 was selected as a maximum limiting factor for sedimentation determinations. Normally, in the photo-extinction technique, measurements were only taken on maximum size particles corresponding to Reynolds' numbers considerably below 0.5.

Stokes' law is concerned only with terminal velocity. After a particle starts to settle a certain time must elapse before the terminal velocity is reached. Fortunately, this time is negligible compared with the settling times involved in particle-size determinations in the subsieve ranges.

The particles should fall as they would in a medium of unlimited extent. The walls of the container should have a negligible effect on the sedimentation velocity. For particles in the subsieve range the walls of the vessels over 1 cm in diameter have little effect. Therefore, in a relative large aerosol chamber, this is of no concern.

According to Reference 12, the maximum volume concentration of particulate materials which can be used without appreciably affecting the sedimentation characteristics seems to $\sim 1\%$. At higher concentrations inter-particle forces can be expected to affect settling.

Although Stokes' law is strictly applicable to perfectly spherical particles, it can be utilized for particles whose maximum-to-minimum-diameter ratio does not exceed 4 (Reference 13). The actual extent of error due to shape is not fully agreed upon by investigators in the field of particle analysis.

Extensive studies have been conducted (Reference 15) regarding the influence of particle shape on the rate of sedimentation. It was concluded that in the viscous flow (Stokes' law) region all reasonably compact (not flat or elongated) particles, would show no tendency to orient while settling, but would fall randomly and at a rate close to that for spheres of the same density and volume. Other workers (References 17 and 18) have investigated sedimentation effects of non-spherical shapes, using cubes, plates, rods, and fractured particles. It is apparent that the agreement is as good for irregular particles as it is for spherical shapes within the limits of shapes investigated.

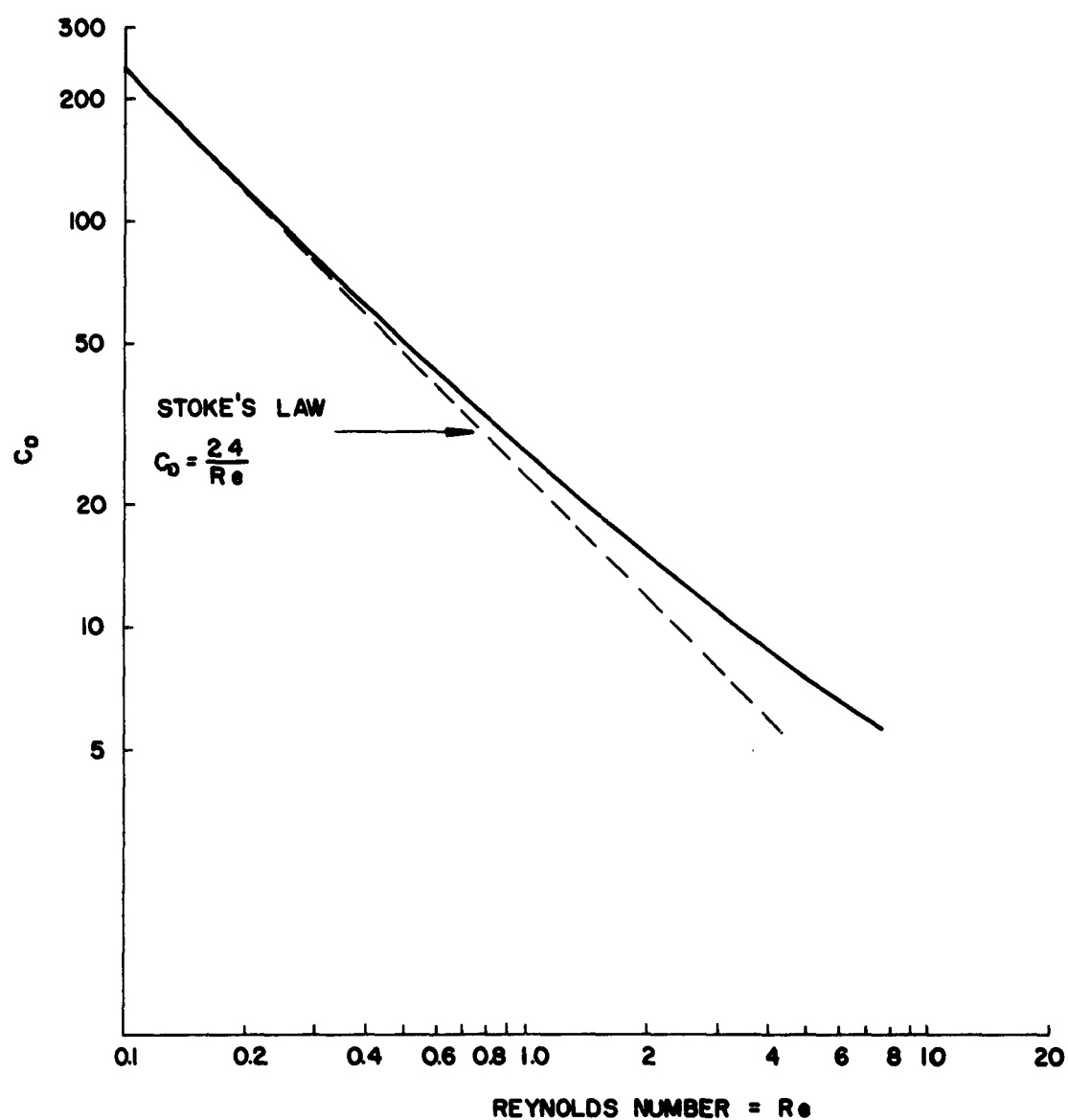


Figure 3. Deviation of Drag Coefficient From Stoke's Law.

2.2.2 Stirred Settling

To achieve maximum homogeneity in an aerosol for greatest reproducibility in measurement, stirred settling has been considered. In stirred settling, the motion of the particles due to convection currents must also be considered. Except for large particles or violent stirring there is little or no impingement on chamber walls or other particles. Essentially, in time, all the particles settle on the chamber floor. The horizontal components of air currents impart no effect on the rate of fall of particles. In a closed chamber, the upward components will compensate for the downward flow components. Therefore, the average rate of fall is the same as that of still settling conditions. The convection currents only maintain a uniform concentration at any given time in the chamber. The relationship of concentration decreasing with time can then be employed to determine size distribution data. Mathematical treatments of stirred settling theory are given in References 19 and 20.

Assuming a monodisperse aerosol in a chamber, the particles obey Stokes' law, and evaporation and coalescence are negligible, then the equations applicable to stirred settling can be developed as follows.

The gas (air) in the stirred chamber can be considered to be composed of small filaments which have either upward or downward velocity components. The total volume rate of flow of the upward elements may be obtained by integrating the upward elements over all their horizontal cross-sectional areas.

$$\text{Volume rate of flow up} = \int_{A_u} S_u dA_u \quad (13)$$

where

S_u = linear velocity up

A_u = horizontal cross-sectional area of upward elements

The total volume rate flow downward then is given by:

$$\text{Volume rate of flow down} = \int_{A_d} S_d dA_d \quad (14)$$

where

S_d = linear velocity down

A_d = horizontal cross-sectional area of downward elements.

In a closed chamber, the net overall volume rate of flow must be zero,

$$\int_{A_d} S_d dA_d - \int_{A_u} S_u dA_u = 0 \quad (15)$$

For an aerosol in the chamber, the linear velocity of the particles in a specific element will be the vector sum of the air velocity and the particle settling velocity. The upward mass rate of transportation of particles is given as:

$$\left(\frac{dM}{dt} \right)_{up} = \int_{A_u} \left(\frac{M}{V} \right) (S_u - s) dA_u \quad (16)$$

where

M = total mass of aerosol in chamber

V = volume of chamber

S_u = upward air velocity

s = Stokes' particle settling velocity

The downward movement of the particles is described as:

$$\left(\frac{dM}{dt} \right)_{down} = \int_{A_d} \left(\frac{M}{V} \right) (S_d + s) dA_d \quad (17)$$

and the net downward movement of the aerosol defines the rate of mass settling on the chamber floor

$$- \frac{dM}{dt} = \int_{A_d} \left(\frac{M}{V} \right) (S_d + s) dA_d - \int_{A_u} \left(\frac{M}{V} \right) (S_u - s) dA_u \quad (18)$$

This expression can be rearranged and substitutions made to yield the following equation:

$$-\frac{dM}{dt} = \left(\frac{A}{V}\right) s M \quad (19)$$

and integrating this gives:

$$\frac{M}{M_o} = e^{-\left(\frac{A}{V}\right) s t} \quad (20)$$

where

M_o = the initial mass of aerosol

t = time of decay

This equation may be rewritten expressing s in terms of the Stokes' radius

$$\frac{M}{M_o} = e^{-\left(\frac{A}{V}\right) k r^2 t} \quad (21)$$

where

r = particle radius

$k = 2 G (\rho_1 - \rho_2) / 9 \eta$

Since aerosols consisting of particles covering a size distribution are of interest, the total mass fraction airborne is given by a sum of terms for each size.

$$F_{total}^{(t)} = \sum_i F_{o_i} e^{-\left(\frac{A}{V}\right) k r_i^2 t} \quad (22)$$

where

$F_{\text{total}}^{(t)}$ = total mass fraction airborne as a function of time

F_{o_i} = mass fraction of particles initially present in the i th class interval.

This expression may be employed with Beer's law, Equation 8, to reduce experimental results into size distributions. The F_{o_i} function however becomes extremely complex and requires a matrix of simultaneous equations for determination. These equations are mathematically unsuited for finding satisfactory solutions when experimental input data are taken into account.

Considering actual test parameters, it is anticipated that ideal stirred conditions are not met because for air velocities small enough to prevent turbulence and impingement problems, the larger particle may not be uniformly distributed in the chamber. This would allow the larger particles to settle more rapidly than the theoretical model predicts, causing a shift of the size distribution toward the larger particles. Stirring is used for attaining greater homogeneity, achieving better reproducibility, and obtaining measurements during the earliest possible period of decay. If the ideal conditions of either tranquil or stirred settling were met, then the theory of sedimentation should also be true for experimental results. In testing practice, neither stirred nor tranquil theory is completely satisfactory in defining existing conditions. The stirred theory may be desirable if a workable mathematical solution is developed. However, since the solution is not available at this time and would require additional work and time, the experimental data in this report has been reduced by the tranquil settling theory. The results from this approach serve as an immediate means for comparing data. Experiments indicate in general that the stirred conditions employed do not cause great deviations from "unstirred" experiments. (see data in experimental presentation). For moderate stirred conditions used at Aerojet, indications are that deviations from theory are small compared to the advantages gained for the technique. Methods of calibrating aerosols of known particle-size ranges may be used to compare results with absolute values to evaluate the effects of actual experimental conditions. This is one more aspect of the photoextinction method that indicates its greatest application may be for relative comparisons of size-distribution information. With the inherent sources of error, it is extremely complex to attempt to control or account for all factors. Nevertheless, the method is considered valuable for obtaining useful information about effect of various mechanisms and parameters of dissemination devices.

3. INSTRUMENTATION

3.1 GENERAL DESCRIPTION

Essentially, the photoextinction apparatus comprises a light source lens with a collimating system on one side of the aerosol chamber and a focusing lens and photographic detector on the other side. The signal received by the photo-detector is relayed to a recorder and a continuous record of the light transmission is made during the decay of an aerosol. In the present system, the output of the light source may also be monitored directly (before the light enters the chamber) by a second photo-detector. This is desirable to detect any fluctuations in the light input. A schematic diagram of the instrumentation system is given in Figure 4. Photographs of the receiver and light source units are shown in Figures 5 and 6 respectively.

Schematic details of the light projector unit, the telescope detector unit, and the electrical circuitry are given in Figures 7, 8, and 9 respectively. The power source used is an E28-30 Nobatron constant-voltage power unit. The unit was operated at 28 v for all measurements. A 28-v lamp (G.E. 1275) is used as the light source. This lamp has a rigidly uniform coil element that withstands extreme shock during the detonation of explosive charges in the chamber.

The two photo-detectors, are diffused silicon photo-duo-diodes, 1N2175, obtained from Texas Instruments Co. (Figure 9). The 2- μ sec response time of the detectors is more than adequate for this application. The spectral sensitivity covers the entire visible spectrum and extends into the infrared region.

The recorder used was a Model 8701061 Minneapolis-Honeywell Recorder with a range from 0 to 25 mv, automatically covered in five steps, expanding the full-scale resolution to 50 in. This corresponds to a deflection of 2 in./mv input signal. The chart speed used is 2 in./min.

3.2 LENS SYSTEM

Normally, in photometric measuring of particles, great care must be taken to achieve collimated light so as to eliminate magnification effects and minimize light scattering problems. It is desirable to reduce alignment variations due to vibrations and thermal changes around the apparatus during tests. The light beam is projected for a relatively long distance making

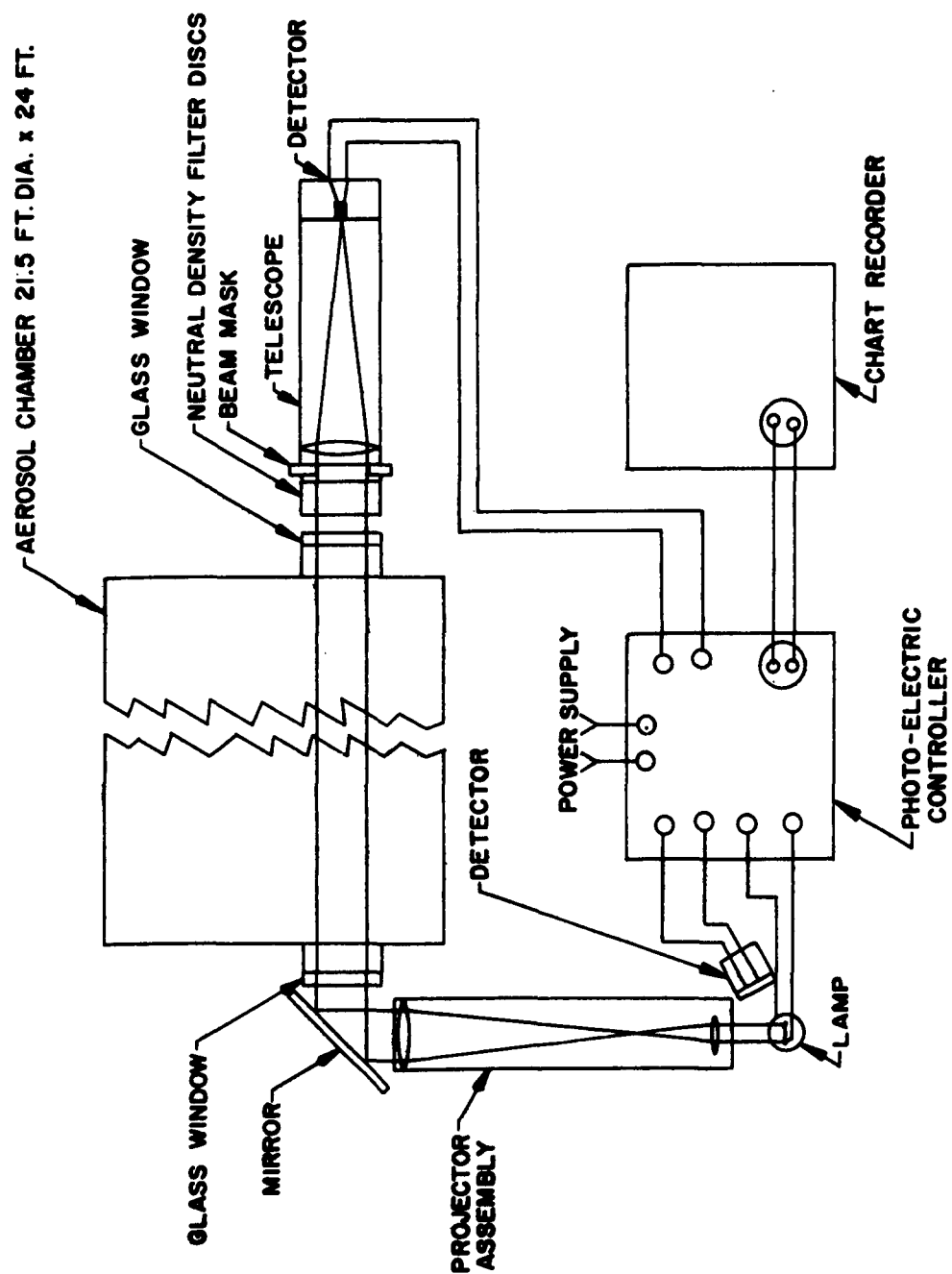


Figure 4. Photoextinction System Composite.

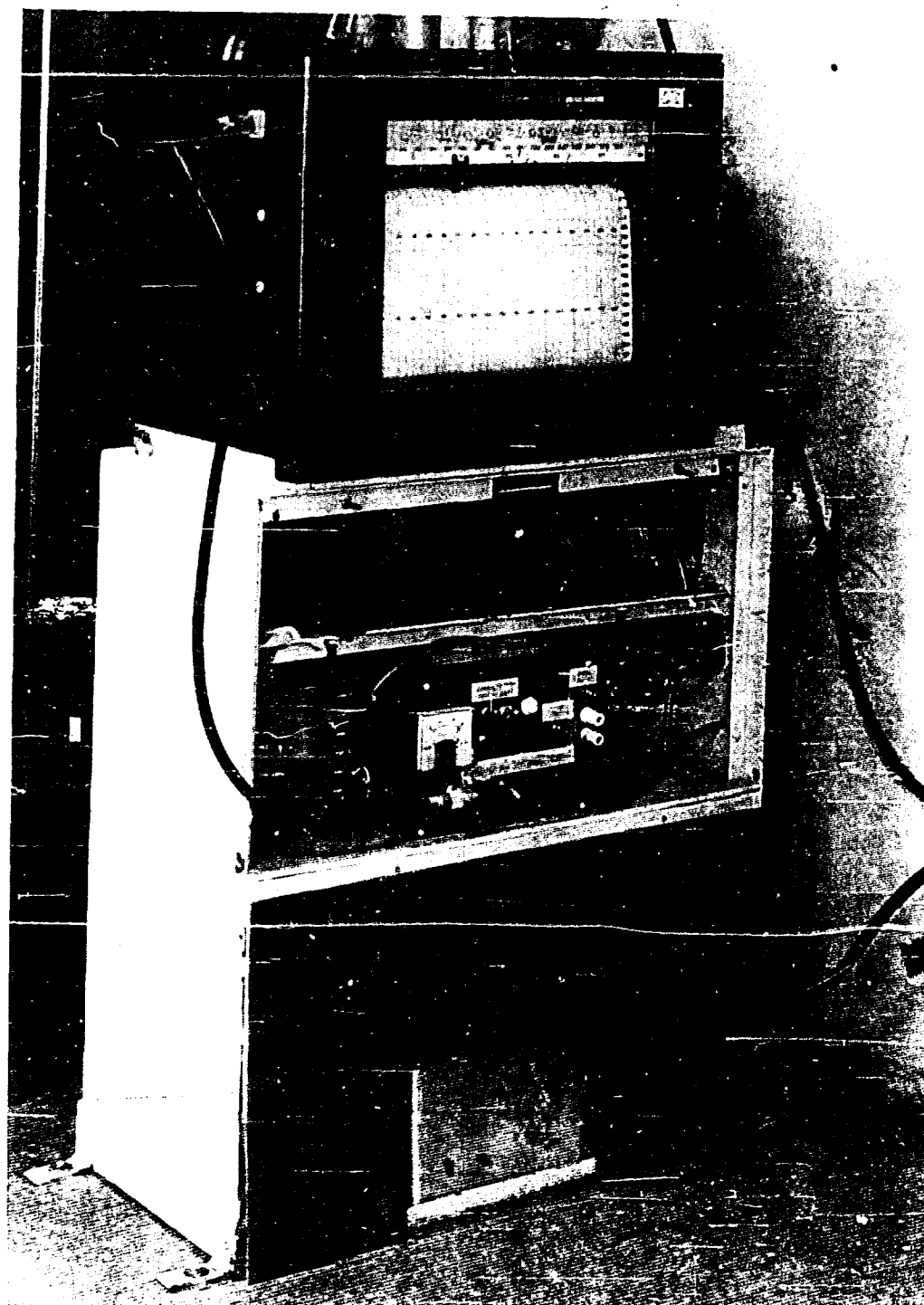


Figure 5. Photostinction Device Receiver

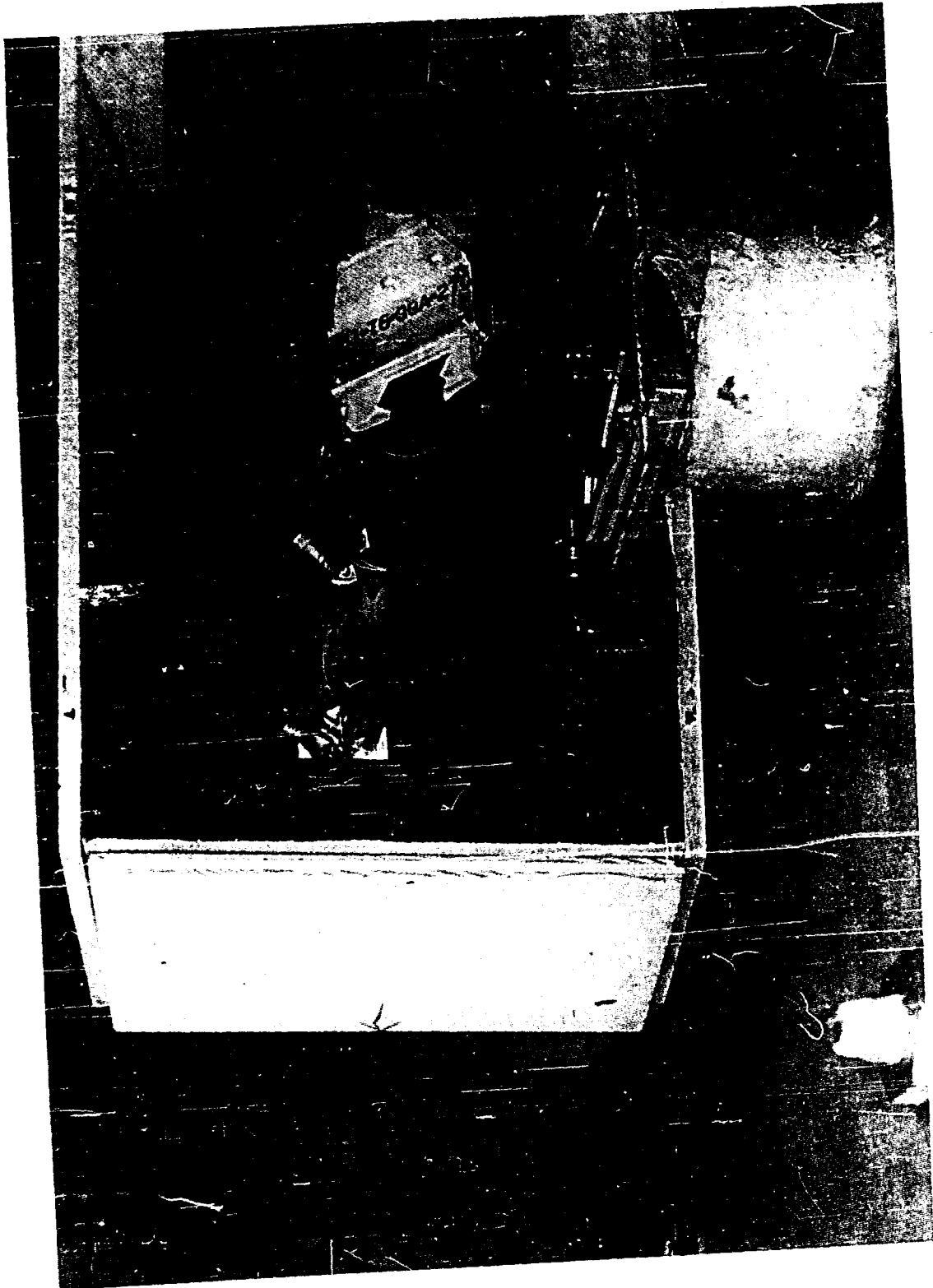


Figure 6. Photoextinction Device - Light Source.

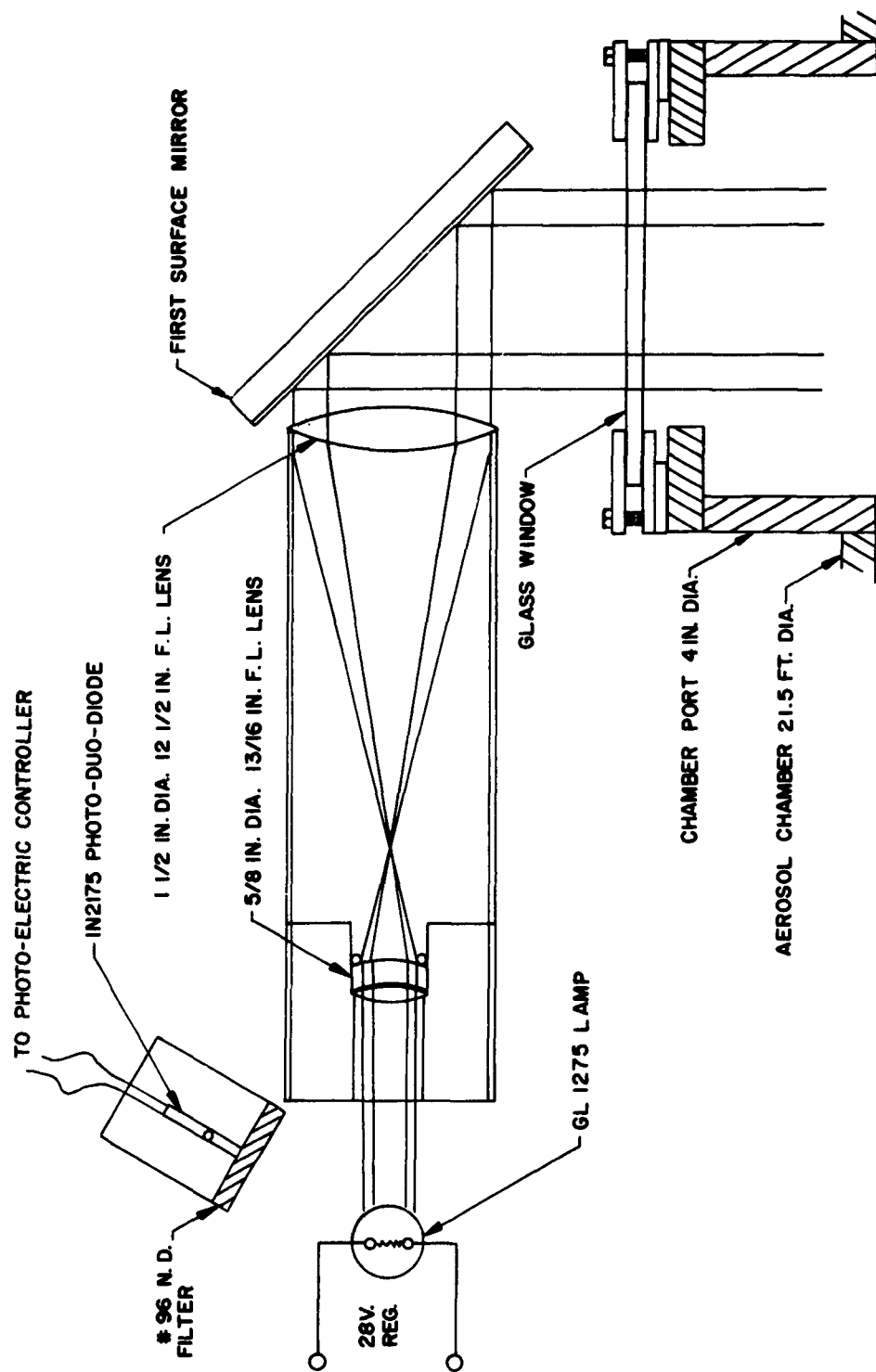


Figure 7. Projector and Window Assembly.

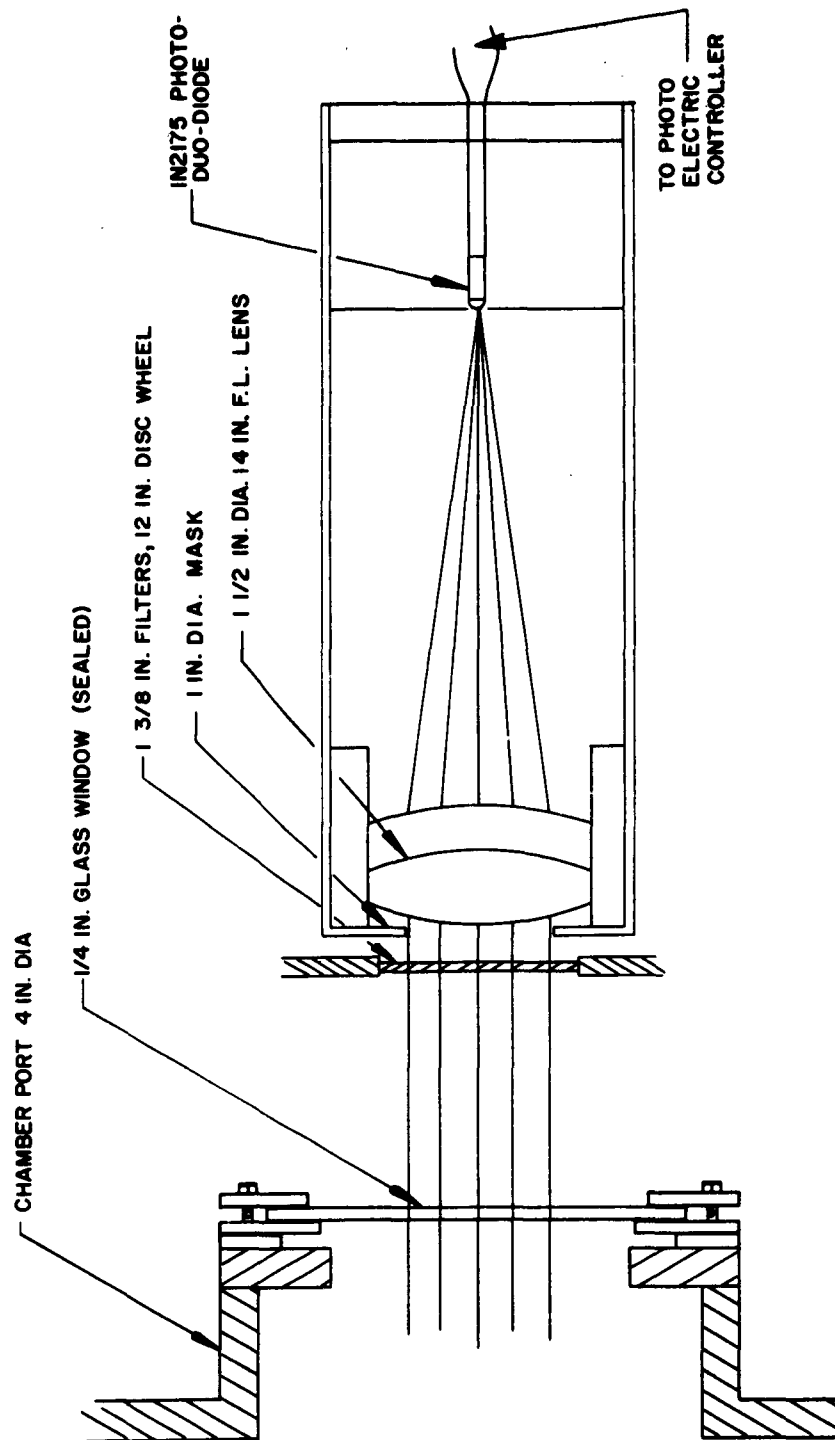


Figure 8. Telescope Detector Assembly.

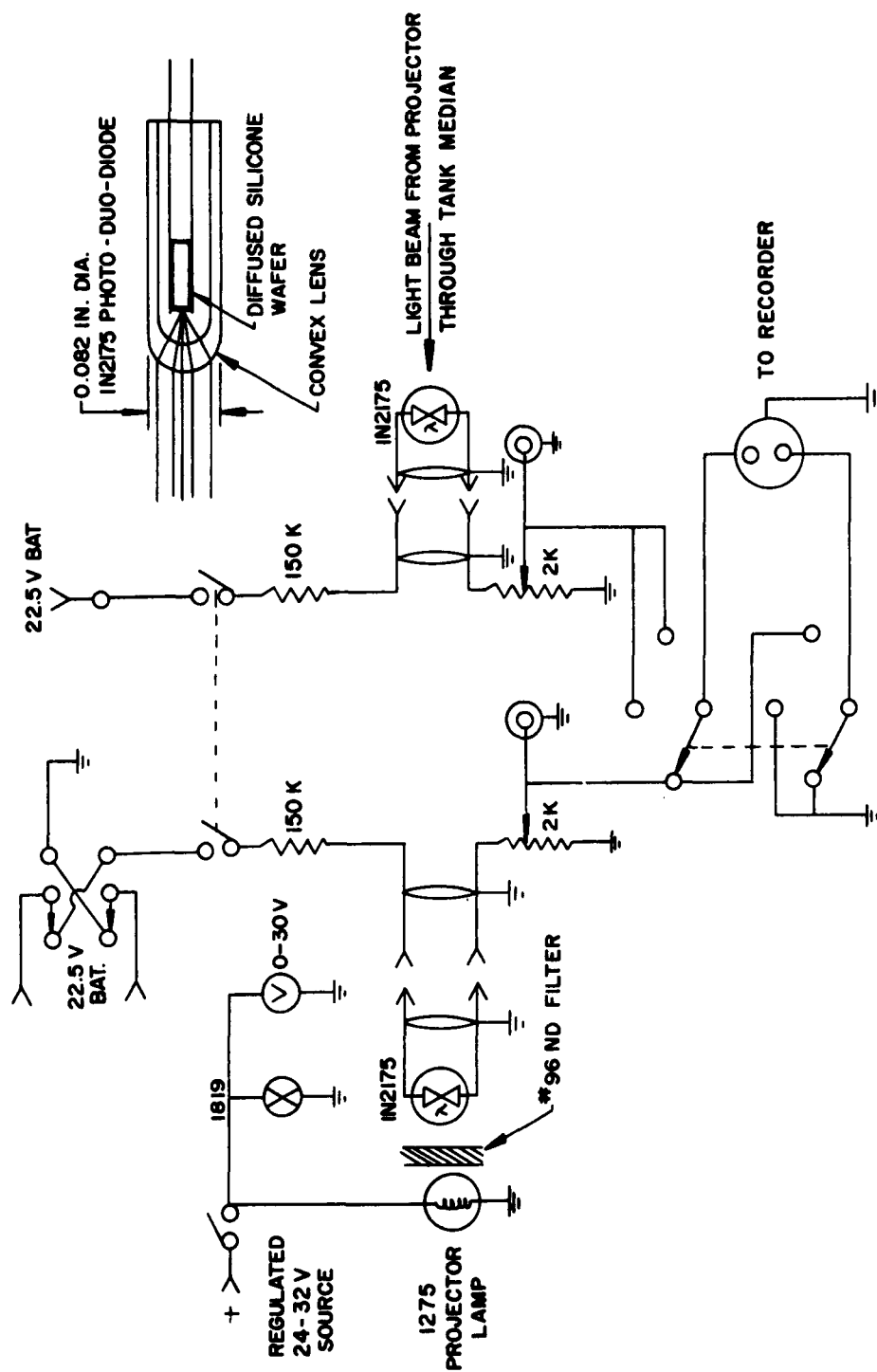


Figure 9. Photoelectric Controller.

alignment sensitive to small mechanical variations at the light source. Also, the period of light transmission recording is relatively long, giving greater opportunity for variations. A solution was to provide a light beam on the emergent side of the chamber with a relatively large cross-sectional area and a constant light intensity over the whole area. The monitor unit can sample a small portion of the beam near the center, and if changes in alignment occur, it should not alter the recorded light transmission. A lack of truly collimated light will not interfere with size-distribution results calculated on a relative basis if the aerosol is initially homogeneous.

Rose states (Reference 11) that light scattering effects are minimized sufficiently if the photo-sensitive surface subtends an angle of 1° or less from the center of the particle being measured. Generally, the transmitted light is focused by a lens onto a photo-sensitive surface beyond the focal point of the lens. A shield with a pinhole aperture is placed at the focal point. The size of the pinhole is small enough to blank out light scattered at angles greater than 1° . In this apparatus the collected light is focused on a small photo-detector instead of passing it through the aperture. The diameter of the photo-detector is small enough to blank out light scattered at angle greater than 1° for particles located anywhere within the chamber.

The "effective" aperture also eliminates non-collimated light from the light source. Light that is not nearly parallel will not be focused on the small photo-detector.

It would be of interest to use a truly collimated light source to compare effectiveness of the small photo diode in eliminating non-parallel light. In this case, the light beam should be of a satisfactory diameter in relation to the beam area measured by the receiver in order to minimize effects caused by alignment variations.

3.3 CALIBRATION

The system is calibrated before each test with standard neutral density light filters. A series of filters are mounted on a rotating disc between the photo-detector unit and the chamber window. Figure 5 shows the disc containing the filters. Readings of the light transmitted through each filter are recorded in duplicates and a calibration curve of percent transmission against chart units is plotted.

Figure 10 shows representative calibration curves from several tests. The shift between the three curves is mainly the result of arbitrarily selecting different 100% transmission scales on the recorder. The lack of linearity at the two ends of the curves is attributed to limitations of the photo-detector. Such limitations are also found in spectro-photometric instruments used in chemical analytical analyses. For practical purposes, the curves are valid in the working light-transmission range.

The calibration filters must be well protected from dust and finger prints to remain accurate. Therefore, the filters were mounted in the instrument console. Total sealing of the filter apparatus would be desirable and might be considered in future improvements.

3.4 INSTRUMENTATION LIMITATIONS

In developing the instrumentation currently used, mechanical and electrical difficulties had to be solved.

3.4.1 Vibration

In preliminary tests, the electronic equipment was either mounted on the steel chamber wall or stood on the floor adjacent to the chamber. The vibrations from the explosive shock perturbed the recorder chart for a few seconds following detonation, and also caused shifts in the standard settings due to slight changes in alignment of the instrument components. This problem was eliminated by bolting the components to the concrete floor.

The initial shock appears to have no effect on alignment, and the transmission values return to within $\sim 2\%$ of the 100% transmission value after exhausting the chamber. Perturbations in the decay curve from the explosive shock vibrations seem minor, since smooth steep curves are obtained during the early decay period in disseminating relatively large particles. However, fine particle clouds exhibit fluctuations in the curve during this early period. This is generally attributed to inhomogeneity of the aerosol. The nonuniform convection currents due to thermal gradients and gas expansion from a detonation do not affect the larger particles as much as the smaller ones. Slow stirring of the aerosol appears to minimize the variation due to inhomogeneities.

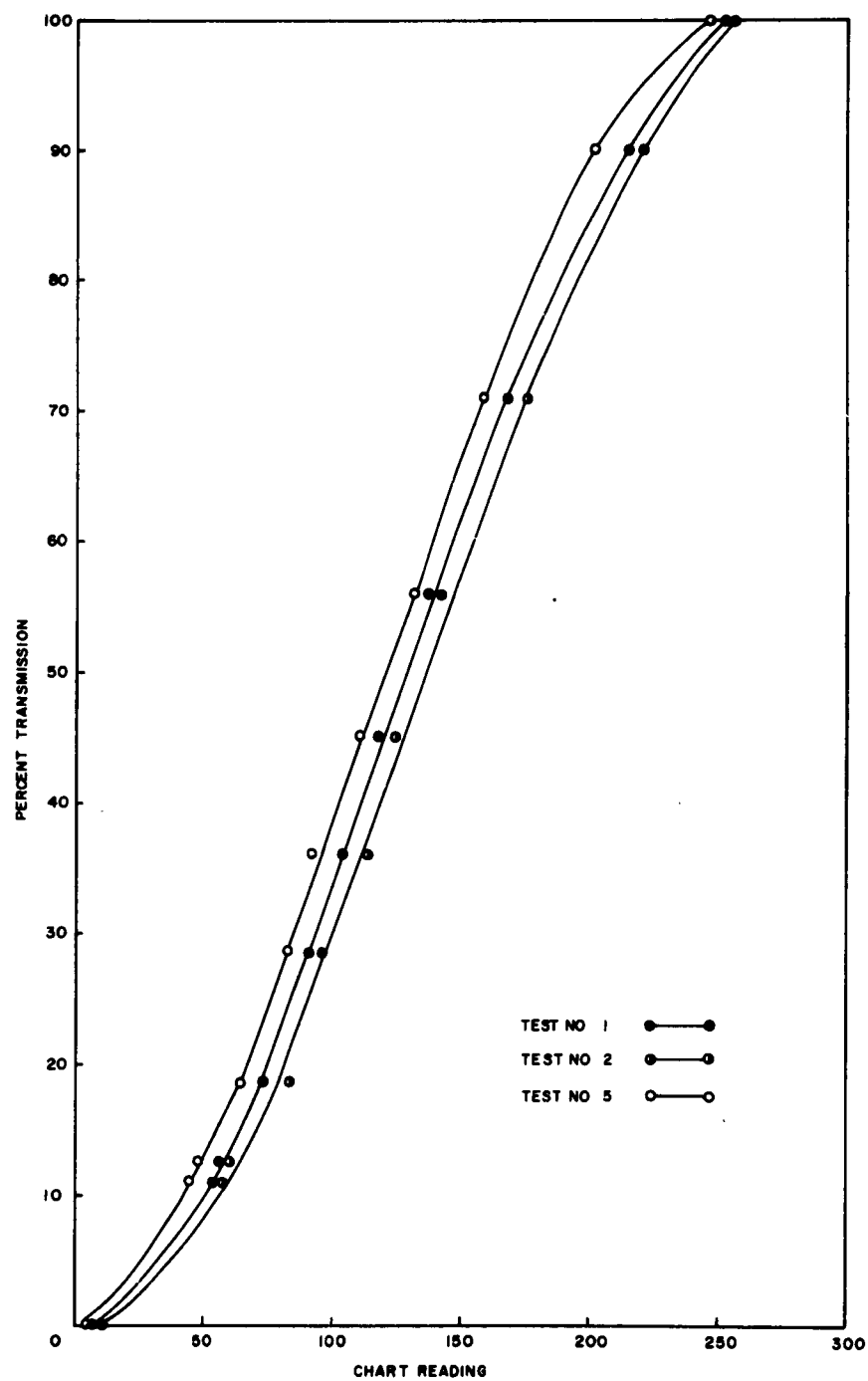


Figure 10. Typical Calibration Curves From Photoextinction Measurements.

3.4.2 Stability of Light Intensity

Over several hours, there appeared to be only a slight change in light intensity due to power-input drift or to tungsten deposition from the filament. The maximum drift noted was $\pm 2.4\%$ over several hours and was normally below this value. To obtain the most reliable data, light-input variations were monitored. Compensations could thus be made in the emerging light intensity values. A second photo-detector was installed to observe the light source before it entered the chamber. The input light intensity could be checked for drift by switching detectors at various times, during the cloud decay. It was anticipated that the second monitor could be coupled with the first to act as a differential readout on the recorder. This coupling was prevented however, by limitations of the electrical system. Another improvement in stabilizing the light source may conceivably be obtained by controlling the light intensity with a photo-detector regulator system.

3.4.3 Temperature Sensitivity

As discussed in Section 3.2, the light source is subject to fluctuations resulting from temperature changes in the surroundings. When air drafts were allowed to inconsistently pass the light source, the recorder measured significant changes in light intensity. The lamp housing was modified to shield it from air currents. However, this shortened the life of the lamp because of inadequate cooling. Because the bulb had to be replaced more often, frequent realignments of the optical system were required. An improved lamp bulb with a longer life (G.E. 1275) was found. Also, the air current shielding was redesigned to prevent direct drafts, but at the same time allowing slow removal of heat by convection currents.

3.4.4 Cloud Density

Photometric measurements are limited by the optical density of the cloud. Relatively high-particle concentrations may block out an excessive portion of the light. In the transmission region below 10%, the instrument lacks the sensitivity to give accurate results. An increase in light intensity would assist in measuring clouds of greater densities; however, it would require considerable expansion of the scale and would be inconvenient to operate. Also, high density clouds tend to increase the error due to particles hiding each other thus cancelling their contribution in light absorption.

Theoretical estimations of light absorption by specific particle sizes have been made. The calculated blocking power appears to be of the order of experimental values observed with the instrument. However, since reliable measurements cannot be made during the first seconds, the maximum density readings are only rough estimates.

3.4.5 Deposition on Chamber Windows

Initially, Plexiglas windows were used to transmit the light beam through the chamber walls. During the aerosol decay, the particles, due to electrostatic attraction, have a tendency to collect on the inside window surfaces. The windows are periodically cleaned during the experiments to ensure reliable readings; as a result significant changes in light transmission have been observed. Plastic is subject to a buildup of electrostatic charges from friction resulting from cleaning. Use of antistatic solutions, such as Dow's Statnol, minimized the electrostatic effects, although they were not completely eliminated. It was also found that different areas of the plastic had a tendency to exhibit nonuniform polarizing effects on the light; therefore, it became critical to replace the windows in their original position after cleaning.

Plate glass windows (1/4 in. thick) were later mounted permanently in place (Figure 6). These windows improved the light transmission and eliminated the positioning of the window after the cleaning operation. A slot was provided so that a steel plate could be inserted between the glass and the disseminator for protection from high velocity fragments during detonation of an explosive device. The shield is inserted before firing and removed immediately on detonation to record data. The slot is sealed after removal to prevent possible air currents from entering the chamber. The same slot is used to clean the window by inserting another shield covered with a pad which rubs the surface of the glass. The pad is treated with an antistatic solution. Using this procedure, there is seldom any significant effect of particles coating the glass.

3.4.6 Homogeneity Aerosol

Inhomogeneity of the cloud in the early stages (first 2 min) of decay makes it difficult to define a consistent decay curve in this region. However, for particle distributions with MMD values of 20μ or less, the majority of the mass is still airborne after 2 min. Therefore, an extrapolation of the transmission curve into the larger particle range (on the order of 50 to 100μ) may be used to some extent, without causing serious deviations in the size distribution curve. A useful indication of the cloud's average optical density during the early period could be realized by momentarily increasing the response time of the photo-detector, thus producing a smoother average curve for any desirable duration.

The homogeneity of the cloud is improved using stirred settling conditions; however, with practical stirring rates, a finite period is still required to achieve suitable mixing of the cloud. The slow stirring rates were chosen to minimize impingement of particles ($>30\mu$) on the four blades.

After 2 min of slow stirring the decay curve generally exhibits a relatively smooth and orderly increase in light transmission. This observation would indicate a near equilibrium in the cross-sectional cloud homogeneity and a lack of significant distortions due to non-uniform convection currents. Experimental effects of slow stirring vs tranquil settling are presented later in this report.

A problem that arises in experimental applications of Stokes' law is that of establishing the height of fall. For a homogeneous cloud completely filling the confines of the chamber, it is clear that the height is measured from the center of the light beam to the top of the chamber. However, all dissemination devices do not produce equally sized clouds due to the energy applied in the dispersion, nor will they fill a large chamber without violent turbulence introduced by stirring techniques. For a given disseminating device, it should be possible to establish an effective height for use in subsequent calculations. However, since numerous device geometries and different energy sources complicate the issue within test series, it was decided to employ a standard procedure height value reaching the ceiling of the chamber. Thus, even though the results become relative, the direction of shift of the size distribution is known, i. e., the calculated particle sizes are larger than the actual particle size. The magnitude of this shift may be calculated for various height values and estimates made for the shift on the basis of information about the specific device. If the cloud could be instantly homogenized and uniformly distributed throughout the chamber this error would be eliminated.

4. DATA REDUCTION

Calculation of particle-size distributions from the experimental data calls for interpretation of the theoretical principles and justification of several assumptions to reduce the procedure for practical use. One method reported by Harner and Musgrave (Reference 14) simplifies the data reduction by using a constant extinction coefficient and calculating a mass proportionality factor for each particle interval from the change in light transmission and the particle diameter. The logarithmic function of light transmission is not used as given by Beers' law. Although the theory is not substantiated, the method gives a rapid means for comparing results in a relative sense. Size distribution data derived by this technique from experimental results are presented for comparison later in this report.

The procedure outlined by Michaels (Reference 14) employs both Rose's extinction coefficient for each size interval and the logarithmic intensity relation in Beers' law. Both of these methods involve calculations of mass relations based on the summation of all the particle intervals. Since the first intervals near $t = 0$ cannot be measured due to turbulence and inhomogeneities, extrapolations to a maximum particle size are made (other methods not requiring extrapolation are described later). Extrapolation may be reasonable for a portion of the curve; however, an arbitrary cutoff or maximum size must be chosen. Particles observed with a microscope can give an approximation of the largest size if it is assumed that the particles have not been significantly altered in handling. This may not be warranted when considering the great amount of agglomeration that can take place in powders. However, to include the contribution of larger particles to the distributions, consistent extrapolating techniques have been explored.

The simplest extrapolation procedure is to extend the curves to a predetermined time representing the maximum particle diameter. Extrapolating by hand appears to give reasonable reproducibility if the extrapolated segment is not great. Plotting the light transmission curve on a semi-logarithmic scale helps in reproducing extrapolations since it approximates a straight line for many tests.

To remove human bias in extrapolating the percent transmission-time, data may be submitted for computer determination of a best-fit curve. Using data from several experiments, the most consistent and usable fits were obtained from the simple polynomial equation $y = A_0 + A_1 x + \dots + A_4 x^4$, where $y = \% \text{ transmission}$, and $x = \text{time in minutes}$.

Utilizing the y intercept, A_0 , of the best-fit curve, a mathematical approach may be used to consistently determine a maximum particle size. The following expression has been derived to standardize calculations:

$$\frac{\log T_{dmax} - \log A_0}{2 - \log A_0} = K \quad (23)$$

where

T_{dmax} percent transmission as the last of the largest particles pass the light beam

K = a constant

The term $(\log T_{dmax} - \log A_0)$ gives a value for the percent transmission adjustment from the theoretical transmission at time 0 to the actual maximum density of the aerosol. The term $(2 - \log A_0)$ serves as a normalizing factor between tests. K must be empirically set and a value of 3×10^{-3} agrees with values obtainable from handcounting of particles. It is recognized that this is a relative procedure: its purpose is strictly to achieve reproducibility in data reduction techniques.

A data reduction method that appears more justifiable is to determine the relative size-distribution curve for the recorded decay curve only. Then Millipore filter samples, taken in duplicate, during a late period of decay may be used to normalize the distribution curve. Thus, the experimentally measured data only are represented in the distribution and no extrapolations are used. This approach depends on the Millipore samples being representative of absolute mass values; the most representative sampling should be possible when only small particles are airborne and the mass concentration is changing at a relatively slow rate.

A graphical method for stirred conditions was proposed for approximating the mass distribution associated with a given decay curve. This method seems adequate for initial comparisons only.

Equation 21 may be rewritten as:

$$\ln m/m_0 = -\left(\frac{A}{V}\right) \frac{K}{4} D^2 t \quad (24)$$

From this expression, when the $\ln m/m_0$ is plotted vs time for a given chamber and disseminated material, the slope of the resultant line is a function of only the particle size. Therefore, the instantaneous slope of the decay curve at some mass fraction can be used as an approximation of the characteristic particle size of the cloud.

The method consists of constructing tangents to the decay curve at various mass fractions. The slopes of these tangents can then be compared to the slopes of a standard plot of Equation 24 for specific material and chamber parameters to determine the particle sizes they represent. These particle sizes can then be plotted vs the mass fractions they represent (mass fraction at point of tangency) to generate the mass distribution curve.

Since, however, the assumptions made by Boyd for stirred settling are experimentally not valid in this study, and the mathematics are extremely complex, Equation 24 was not employed in the data reduction. With further work, it may be possible to develop a mathematical program based on stirred settling theory which will account for the true conditions. However for comparison purposes, the still settling theory was applied. This application provides a relative and useful tool for assessing dissemination experiments and microscopy evaluation seems to give particle size values close to the actual dimensions.

5. ERROR EVALUATION

Quantitative evaluation of the possible errors in the photoextinction system would be extremely complex since errors depend on such parameters as particle diameter, physical and chemical properties, and existing conditions. A qualitative analysis can be made however, where problems can occur.

Specific theoretical and instrumentation problem areas have been mentioned. Means of accounting for, or compensating for, these problems were also presented. Therefore, to minimize errors, the following conditions will be assumed.

- a. The photographic receiver subtends a sufficiently small angle with all particles to limit errors due to forward light scattering.
- b. The refractive index between the particle and the medium is great thus the particles will behave as though they were opaque.
- c. The general shape of the particles does not deviate from spherical geometry by more than a 4:1 ratio for the maximum to minimum dimensions.
- d. The maximum particle size measured falls within the set limit according to an acceptable Reynolds' number.
- e. Roses' extinction coefficient accurately corrects the hiding capacity of particles of all sizes in the range being measured.
- f. Errors in drag coefficients due to wall effects are negligible for large test chambers.

For Reynolds' numbers of the order considered, an error $\sim 6\%$ smaller than the absolute particle diameter may be expected. However, this error decreases when measuring subsequent decreasing particle-size intervals.

The assumption that the height of fall in the chamber is the ceiling-to-light beam distance, will introduce a one-directional error. If the maximum height of the cloud is less than this height of fall, it will shift the distribution curve to larger particle sizes following Stokes' equation, Equation 10. The magnitude of change in particle size varies with the square root of the height of fall. An effective height may be estimated from empirical evaluations of standard particles for specific dissemination devices.

Agglomeration may cause deviations in size measurements in several ways. The particles of an aerosol may contain solid particles and agglomerates of identical size, but due to differences in effective densities, they will have different settling velocities. Therefore, the agglomerate will fall more slowly and will be included in measurements corresponding to smaller diameter particles. This results in a shift of the distribution curve to smaller sizes. Since electrostatic forces are present, a great deal of agglomeration may take place during the decay process. At some time during settling, small particles may clump, thereby reducing drag and allowing an increase in settling velocity as compared to the individual components. The result is that the fine particles are removed from the aerosol at a more rapid rate causing a shift to larger particles in the determination. Another factor in photoextinction is that, when these particles agglomerate, a relatively large portion no longer absorb light because they are hidden by other particles in the clump. The effect becomes one in which the representation of mass in the fine particle ranges is diminished and thus the distribution curve is again biased by apparently increasing the larger particles relative concentration.

For effects encountered from agglomeration, what is actually to be measured might be considered. Since the agglomeration occurs, it shall be more important to determine the ultimate effects rather than the distribution of the initial aerosol. The effectiveness of an aerosol depends upon cloud stability regardless of its parameters at time 0. Accurate assessment or even a description of the aerosol including the dynamic parameters during its life would be very complex. In this instance it may be mandatory to accept the compromise that these effects would generally compensate each other. Studies of electrostatic agglomeration during cloud decay should offer helpful information to better evaluate experimental data.

Diffusion effects by Brownian motion essentially shift distributions to the finer sizes by slowing settling of small particles. However, for particles of 1μ dia or greater, there is no significant effect.

Some workers contend that the errors generally compensate each other. This is indicated to a degree for some of the experimental work at Aerojet by good correlation obtained between assessment techniques. However, other test data do not agree. Therefore, from the available information, an overall statement describing the extent of errors cannot be made. Errors probably depend upon specific parameters in each series of experiments and may have to be resolved on an individual basis.

6. EXPERIMENTAL RESULTS

The data reduction methods discussed have been applied to measurements made in dissemination experiments. A good deal of the data was treated with the Harner and Musgrave method in earlier work because of the simplicity and convenience of rapid data reduction. The extrapolation methods were varied between the hand-drawn curves and mathematical best-fit curves. Reproducibility by any of these procedures appeared to be subject to differences between a specific series of tests. This indicated that a method excluding extrapolation would be desirable. It was felt that a relative distribution curve based on the measured points with a mass normalizing factor would have its advantages.

The following discussion presents typical results of some experiments. Most of the tests were not designed for studying the photoextinction method; however, they served to compare results of the technique for different materials disseminated under different conditions.

The test chamber was a cylindrical steel tank 24 ft high by 21.5 ft in dia, with four fans in the ceiling. The chamber is enclosed in an air-conditioned building.

6.1 G S SERIES

To establish the range of cloud densities which can be assessed by the photoextinction technique, a series of varying size spherical explosive devices was fabricated with constant filler-burster mass ratios of ~6:1. Silica powder, Minusil-10 (Pennsylvania Glass Sand Corporation) was used as the filler. The Harner and Musgrave method was used to reduce the data resulting in the curves presented in Figure 11. In the higher density aerosols, the decay curves were initially in the low transmission range (below 10%). The lack of sensitivity and possibly the hiding factor caused the shift in the distribution curves toward smaller particles as the cloud mass was increased. Approximations made from the initial size distribution of the silica indicate that a minimum transmission for 70 gm of powder should be ~20%. The earliest measured transmission values (1 to 2 min) fall in an approximate range of 15 to 30% transmission. Further details of this series of tests are given in Reference 21.

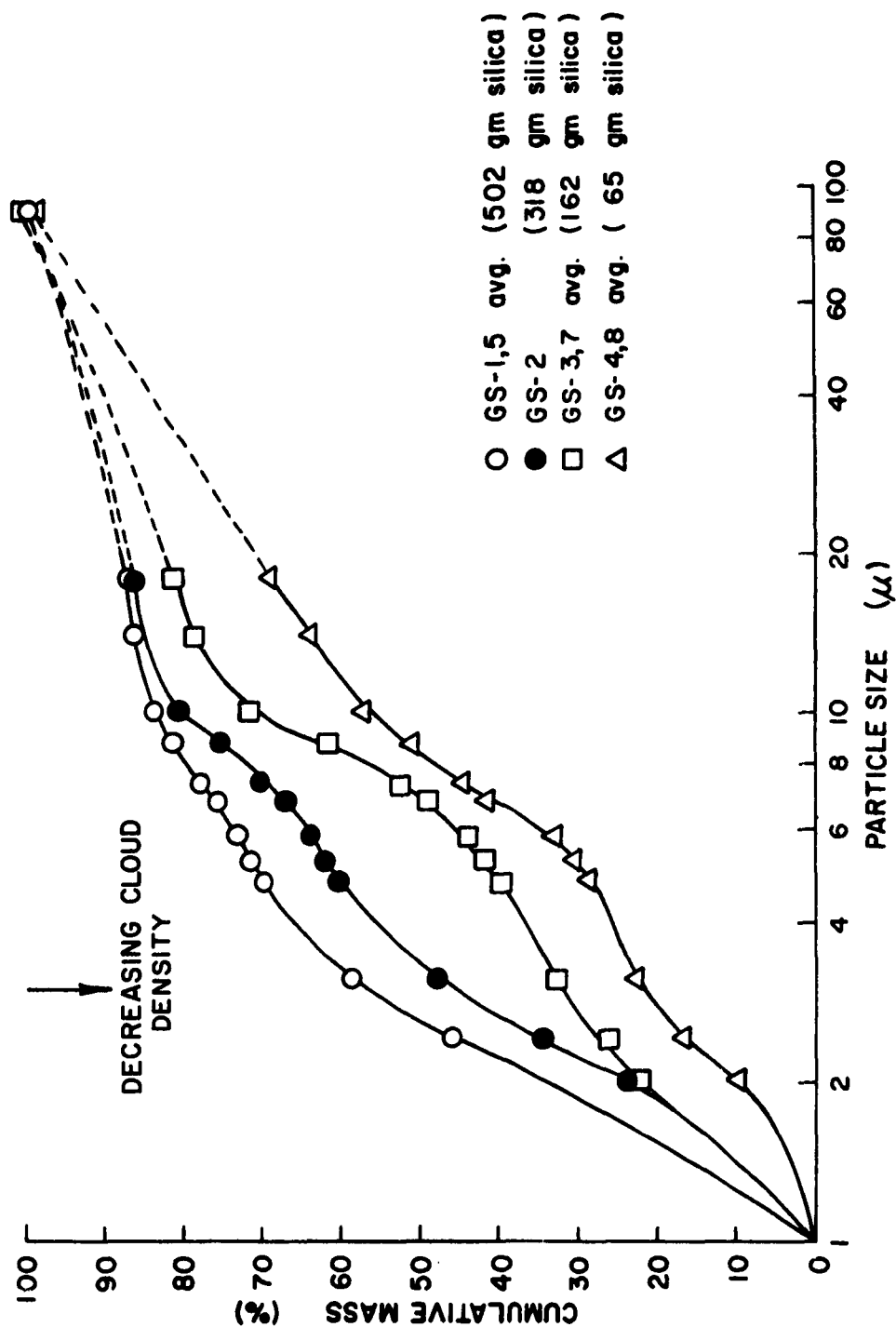


Figure 11. Mass Effect for Silica on Photoextinction Size Distribution Curves.

6.2 D B SERIES

To calibrate or compare results from tests in the Aerojet chamber and those at CRDL, a series of identical explosive-dissemination devices were used in both facilities. Granular sodium chloride ground to a powder with an MMD of $\sim 40\mu$ was used as the filler in the devices. The explosive devices were spherical with a central burster. The parameter variables resulted in filler-burster ratios of from 0.65 to 8.2. A more detailed description of the experiments is given in Reference 21.

In these tests the photometric measurements made were in a transmission range of good sensitivity since the particle size is considerably larger than the silica in the GS series. However, the large particles had a higher settling velocity indicating that the measurable portion of the decay curve represented a substantially lower percentage of the initial particle mass, i. e., the large particles settled past the light beam in the first minute or two before recordable measurements could be obtained.

The transmission decay curves for the series are shown in Figure 12. In Figure 12, the duplicates correspond to the input mass and the data are generally reproducible.

From microscopic observations it appeared feasible to set a maximum particle size and extrapolate the curves by the Harner and Musgrave method. The curves generated for duplicate shots are presented in Figures 13 through 16. The averages of the duplicates are compared in Figure 17. Calculation of the curves could not be calculated by Michaels-Millipore method due to anomalies in the Millipore results.

Although this assessing method measures the aerosol during actual decay, these results were compared to those obtained by micromerograph and the Mine Safety Appliances (MSA) Particle-Size Analyzer. These three methods generally gave similar values. The reproducibility of the photoextinction data suggests a satisfactory relative comparison of experiments.

6.3 PX SERIES

Experiments were carried out in which liquids were aerosolized by injection into a hot-gas stream. A solution of ~ 60 gm Uvinul, (2, 6-dihydroxybenzophenone) in Bis, [bis-(2-ethylhexyl) hydrogen phosphite] were injected into a controlled stream of hot gas directed into the aerosol chamber. Three different sets of parameters were employed to compare reproducibility and trends using the photoextinction technique.

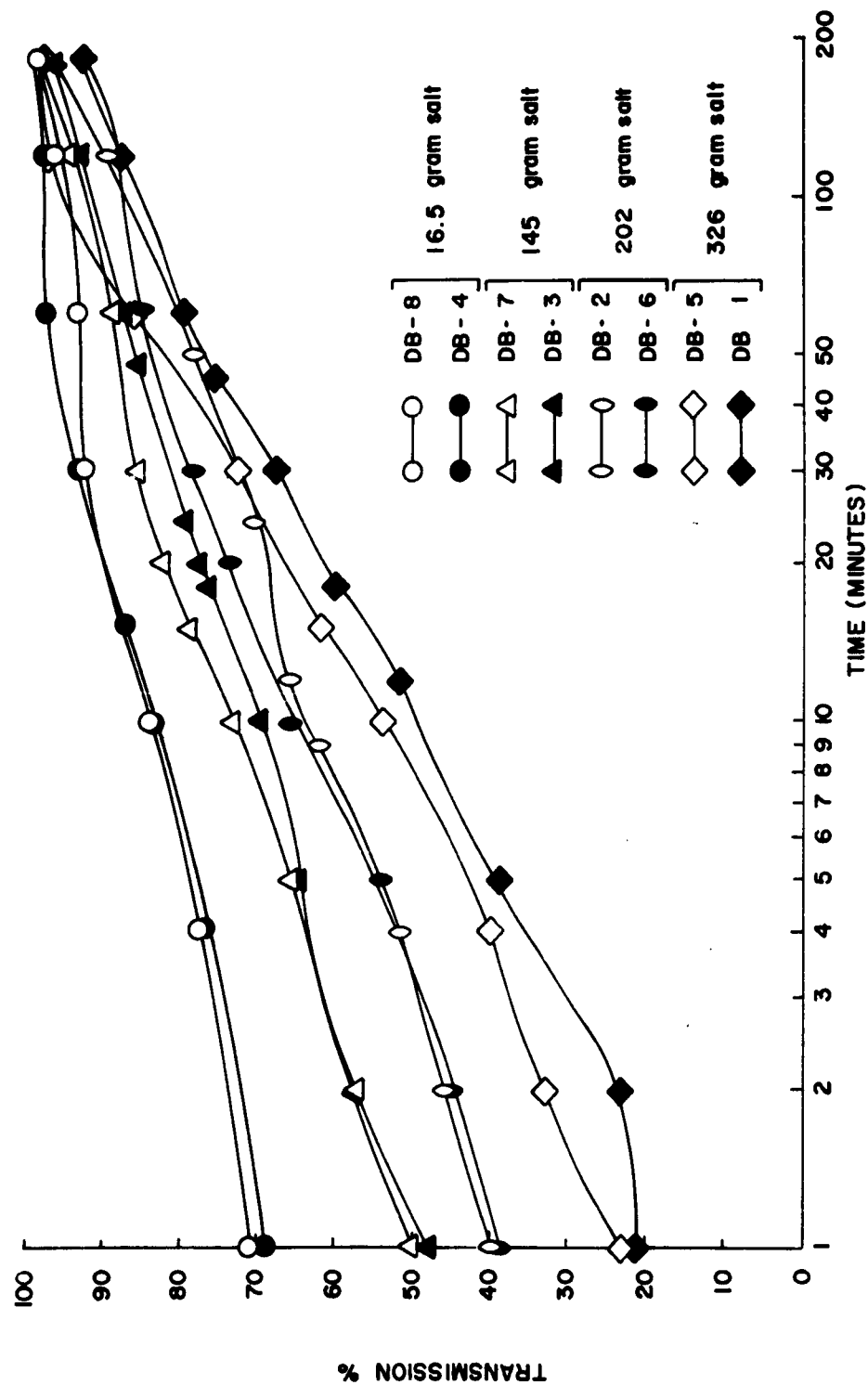


Figure 12. Transmission Curves for DB Series.

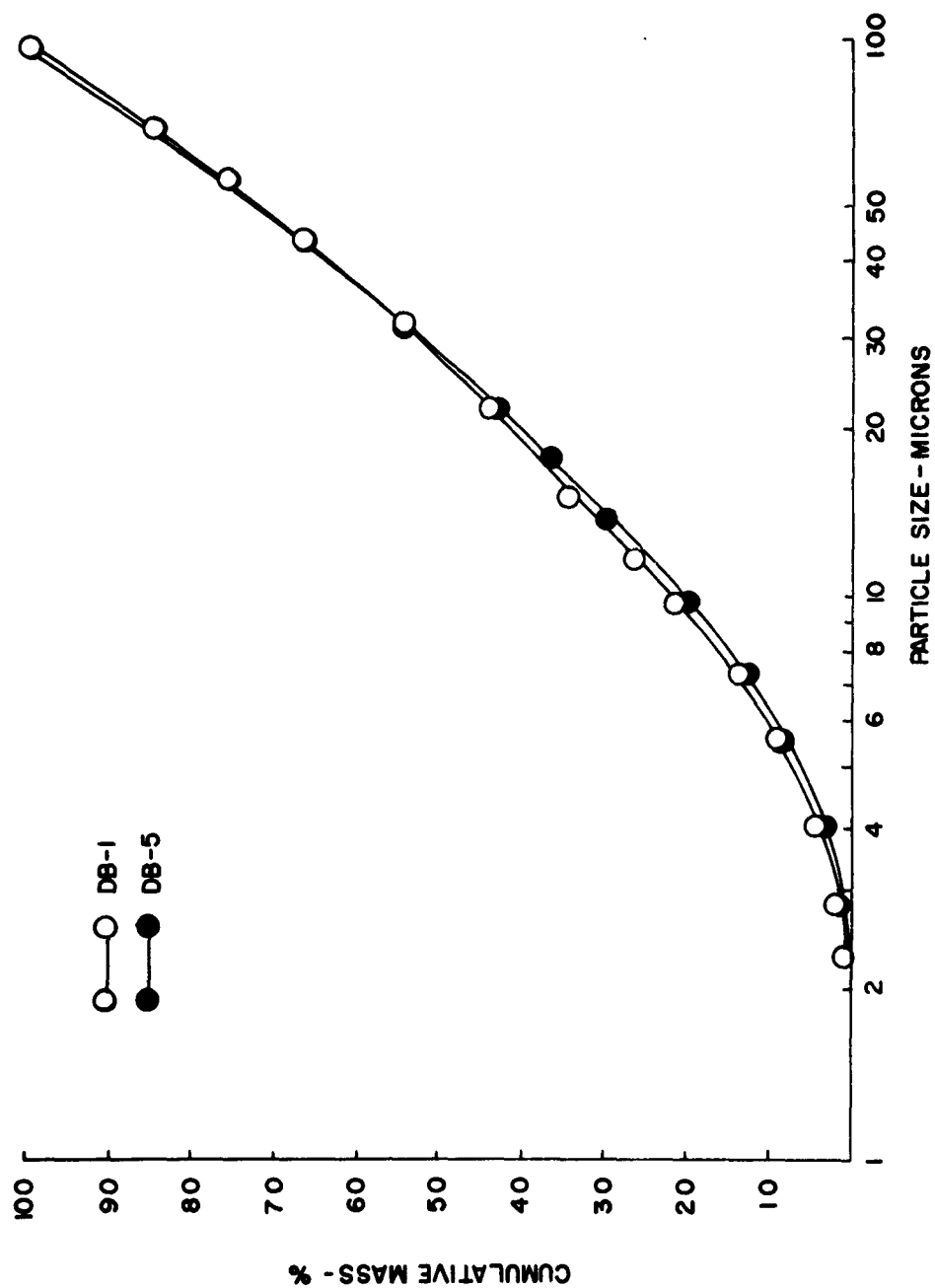


Figure 13. Size Distribution for Salt by Photoextinction, Harner and Musgrave Method (a).

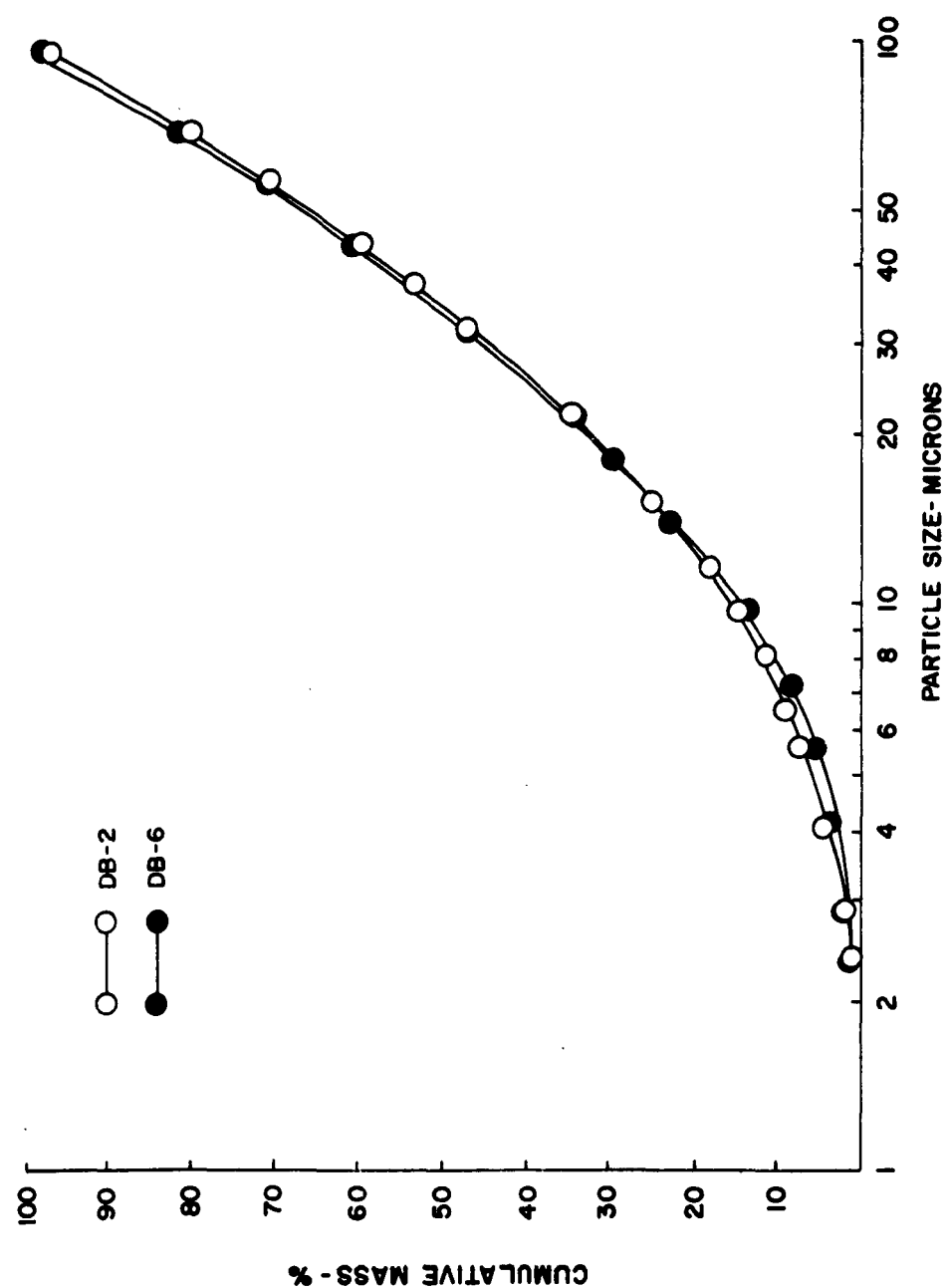


Figure 14. Size Distribution for Salt by Photoextinction, Harner and Musgrave Method (b).

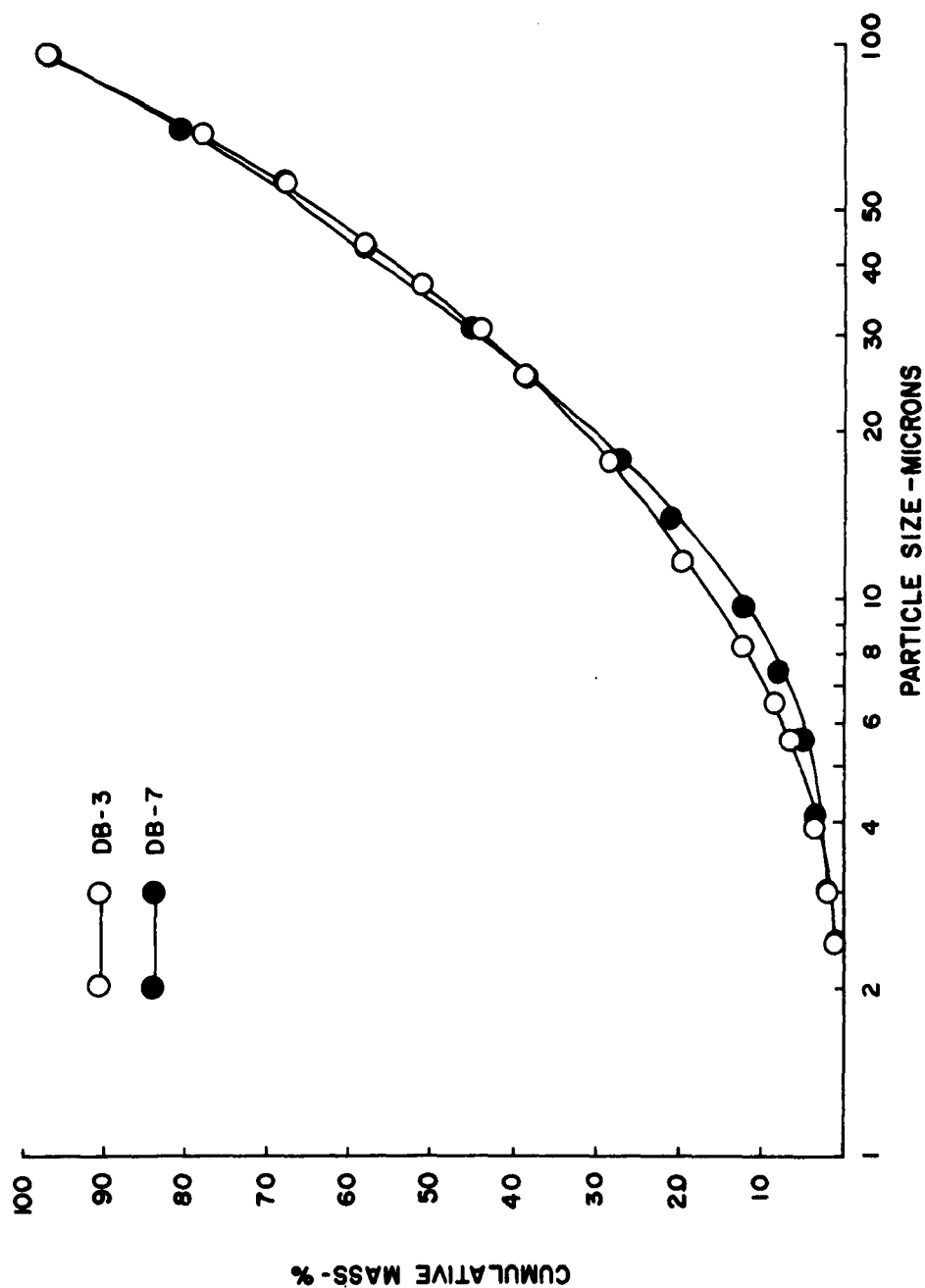


Figure 15. Size Distribution for Salt by Photoextinction,
Harner and Musgrave Method (c).

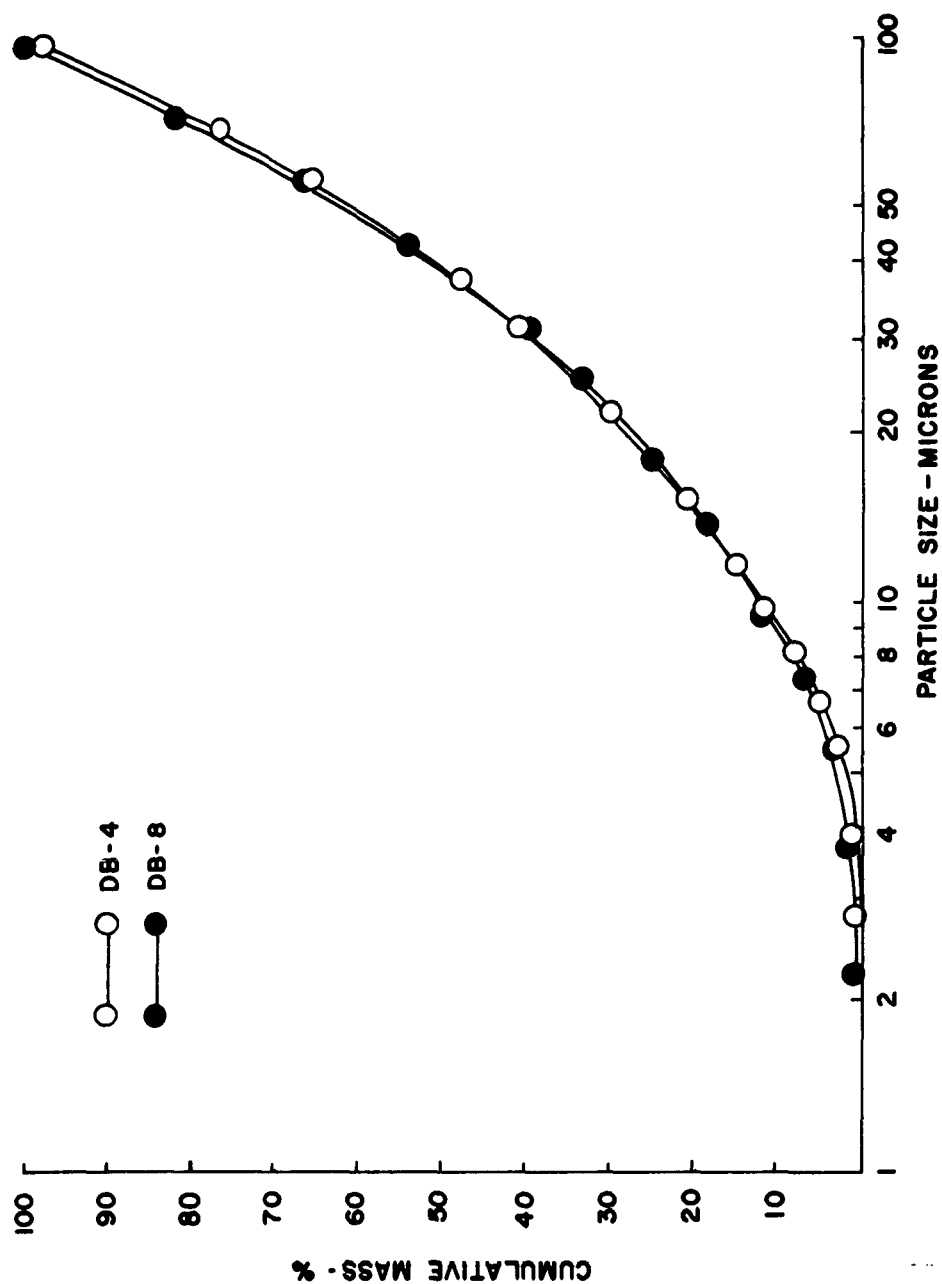


Figure 16. Size Distribution for Salt by Photoextinction,
Harner and Musgrave Method (d).

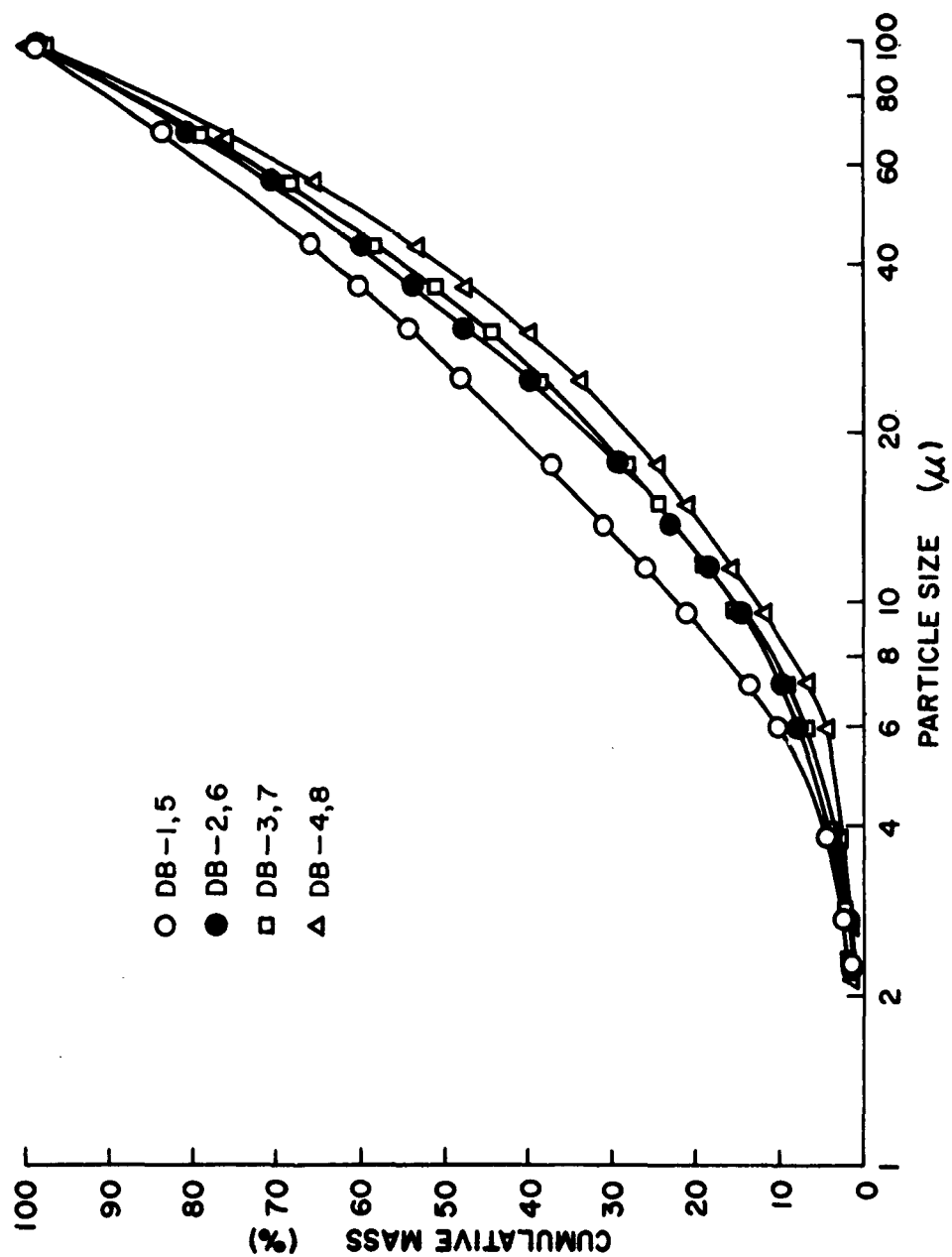


Figure 17. Average Size Distribution Curves for DB Salt Series, Photoextinction, Harner and Musgrave Method.

The Harner and Musgrave method was used for the calculations since no Millipore filter samples were taken. Figures 18, 19, and 20 show the resulting size distribution curves. Conditions 1 and 3 employed single injectors while Condition 2 used a triple injector system. Results using the triple injector show somewhat higher variation than that exhibited by the single injectors. Curves for each condition (1, 2, and 3) are replicates except for stirring where designated.

The difference between stirred- and still-settling conditions does not appear to be the cause for the spread in results. The data are not extensive enough to support strong conclusions regarding specific parameters; however, the reproducibility of the size-distribution curves indicates considerable promise for application to aerosols generated by hot and cold gas dissemination techniques. The small size of the particles and relatively low density of the liquid provided favorable parameters for the photometric measurements of the major portion of the mass input.

6.4 FP SERIES

Other tests were performed with silica (Reference 21) for comparison of settling conditions and data reduction techniques. Spherical explosive devices were constructed containing 60 to 70 gm of silica powder, Minusil-10, having an MMD of 6.5 to 7.5 μ for the unshocked material as determined by MSA and Micromerograph. The explosive weight gave a filler/burster ratio of $\sim 5:1$.

The Harner and Musgrave method was applied to the test results giving the curves shown in Figure 21. With the exception of one test, the distribution curves show good reproducibility for both stirred- and still-settling methods.

Two of the tests for still settling are compared by both data reduction methods (Harner and Musgrave and Michaels-Millipore) in Figure 22. Two tests are compared similarly for stirred-settling condition in Figure 23. These results show the general agreement between stirred- and still-settling conditions. The two data reduction methods also correlate satisfactorily for these tests.

Another series of experiments with silica was conducted to investigate the effect of silicone coatings on the size distribution of agglomerates after aerosolization. The explosive devices were similar to those in the FP series. Using the Harner and Musgrave method, the distribution curves were determined for three treated and three untreated silica fillers.

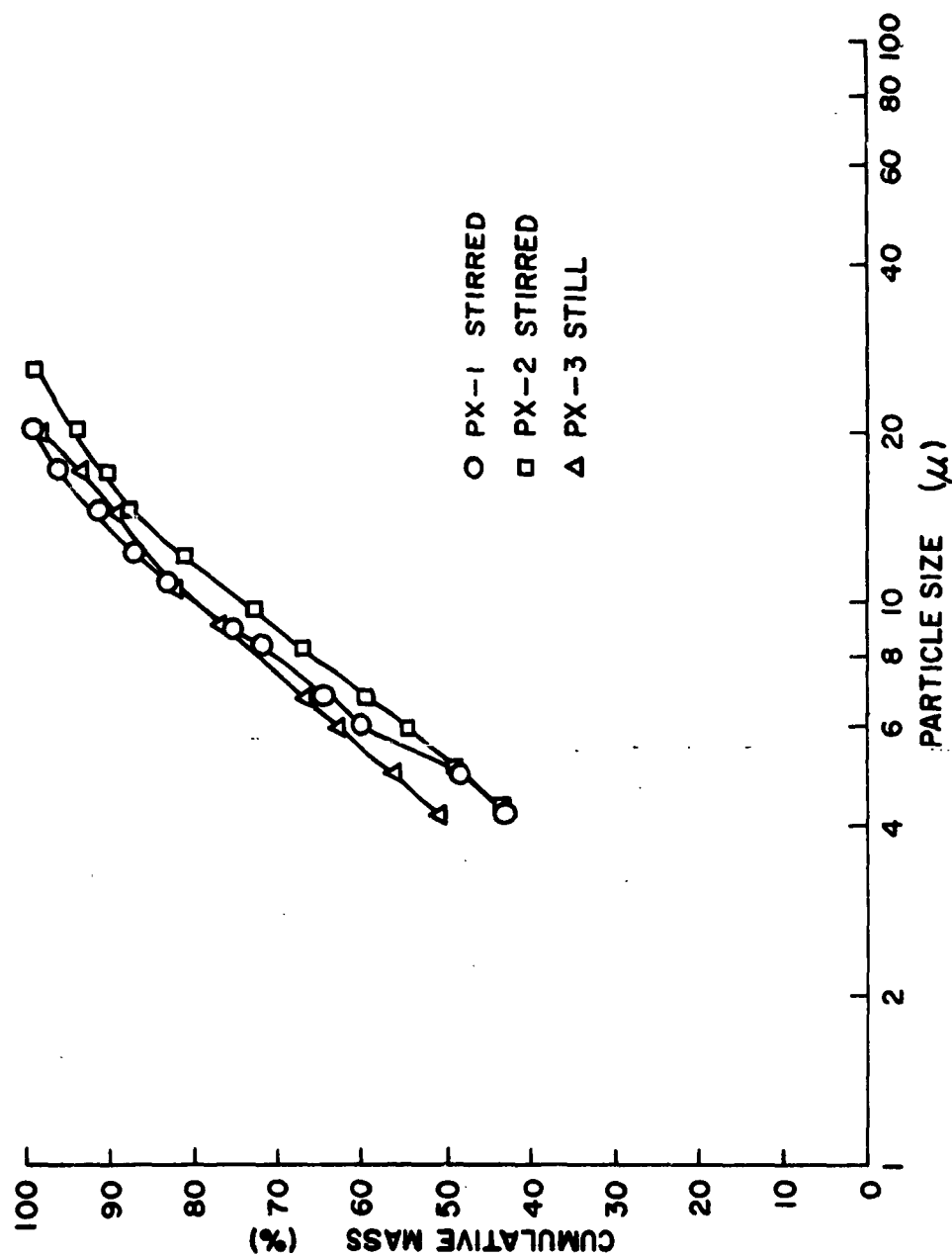


Figure 18. Size Distributions of Bis-Uvinul Solutions, by Hot-Gas Dissemination, Harner and Musgrave Method, Condition 1.

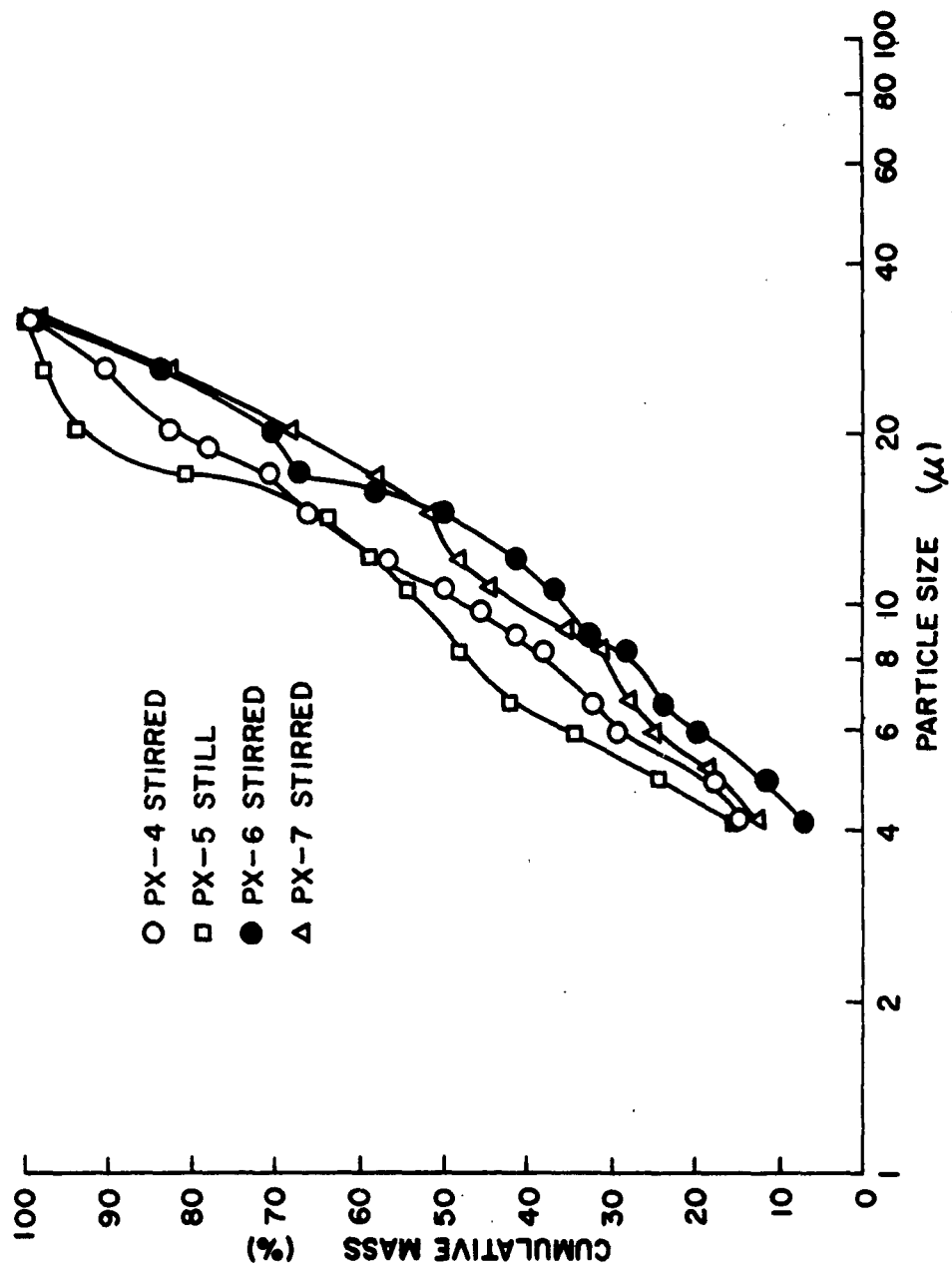


Figure 19. Size Distributions of Bis-Uvinul Solutions by Hot-Gas Dissemination, Harner and Musgrave Method, Condition 2.

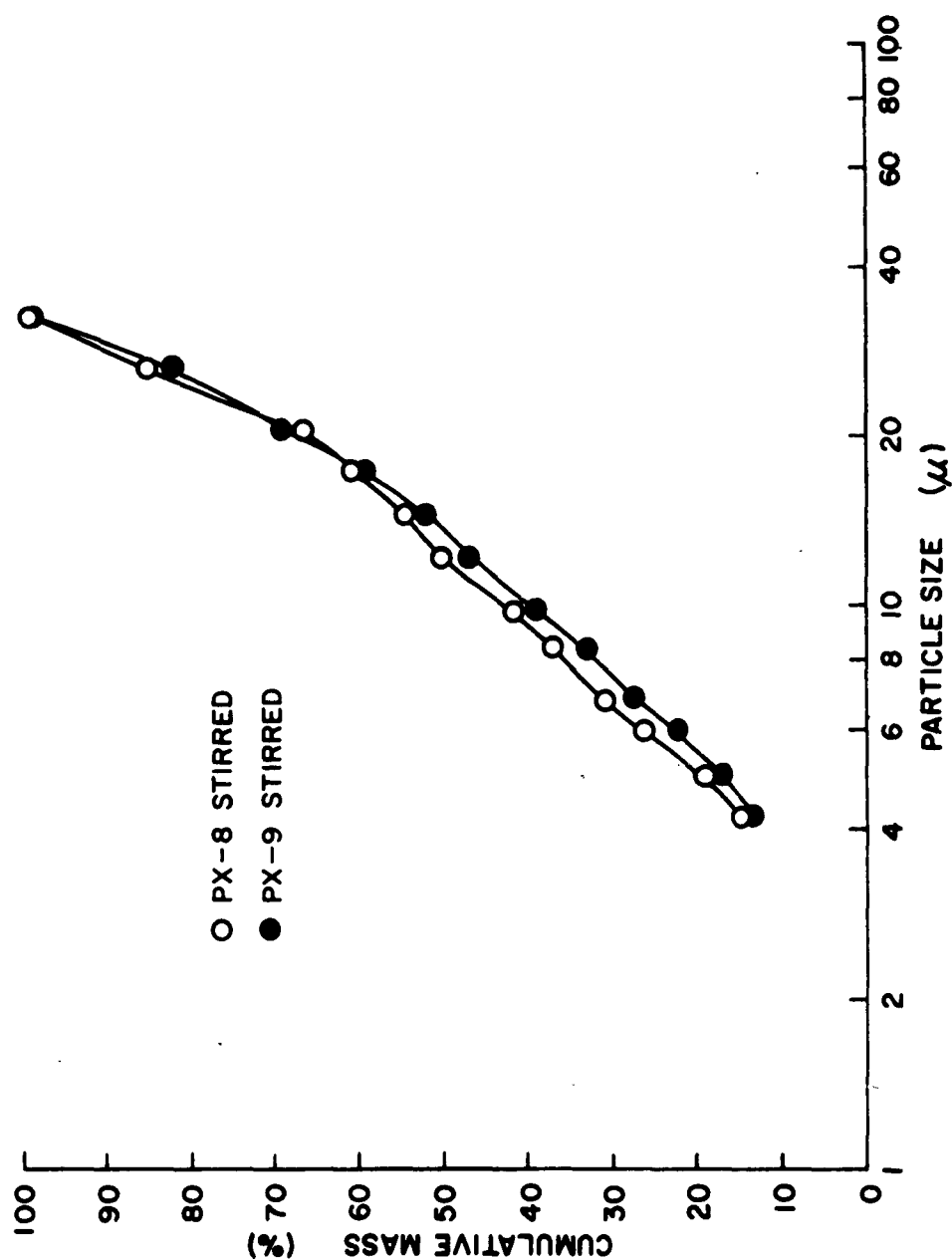


Figure 20. Size Distributions of Bis-Uvinul Solutions by Hot-Gas Dissemination, Harner and Musgrave Method, Condition 3.

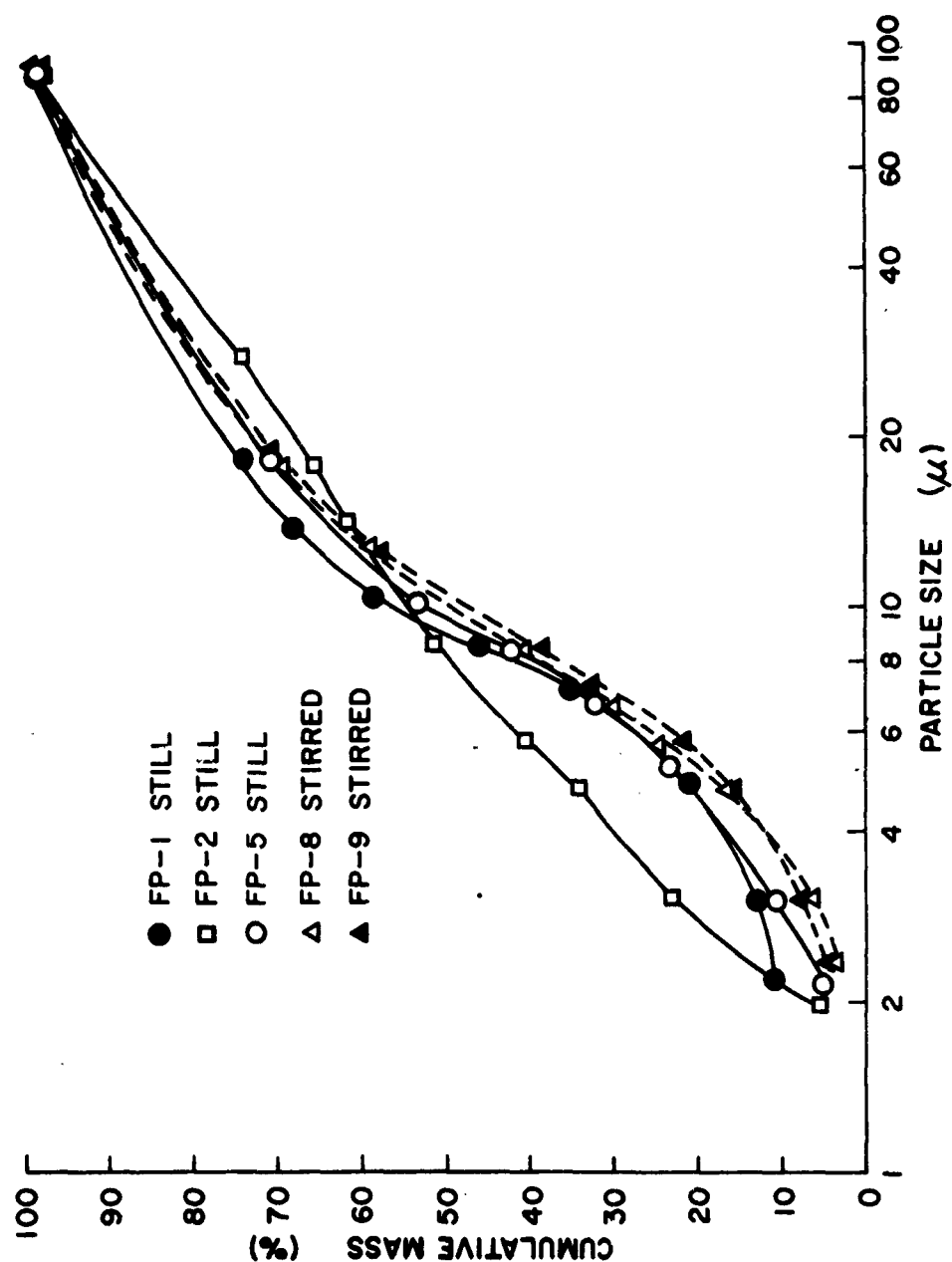


Figure 21. Size Distribution Curves for Silica From Photoextinction, Harner and Musgrave Method.

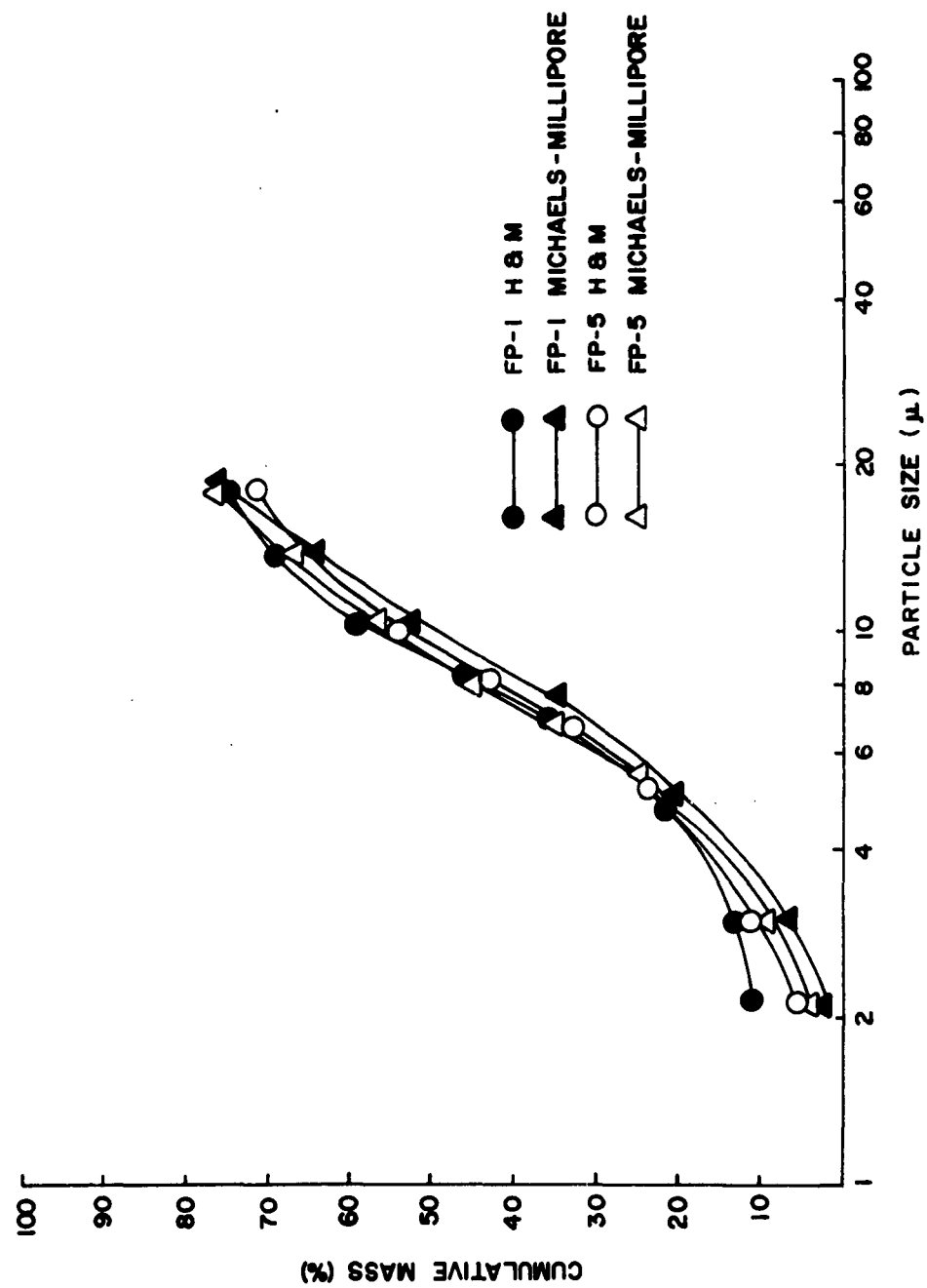


Figure 22. Data Reduction Comparison of two Methods - Still Settling, (1) Harner and Musgrave, and (2) Michaels-Millipore.

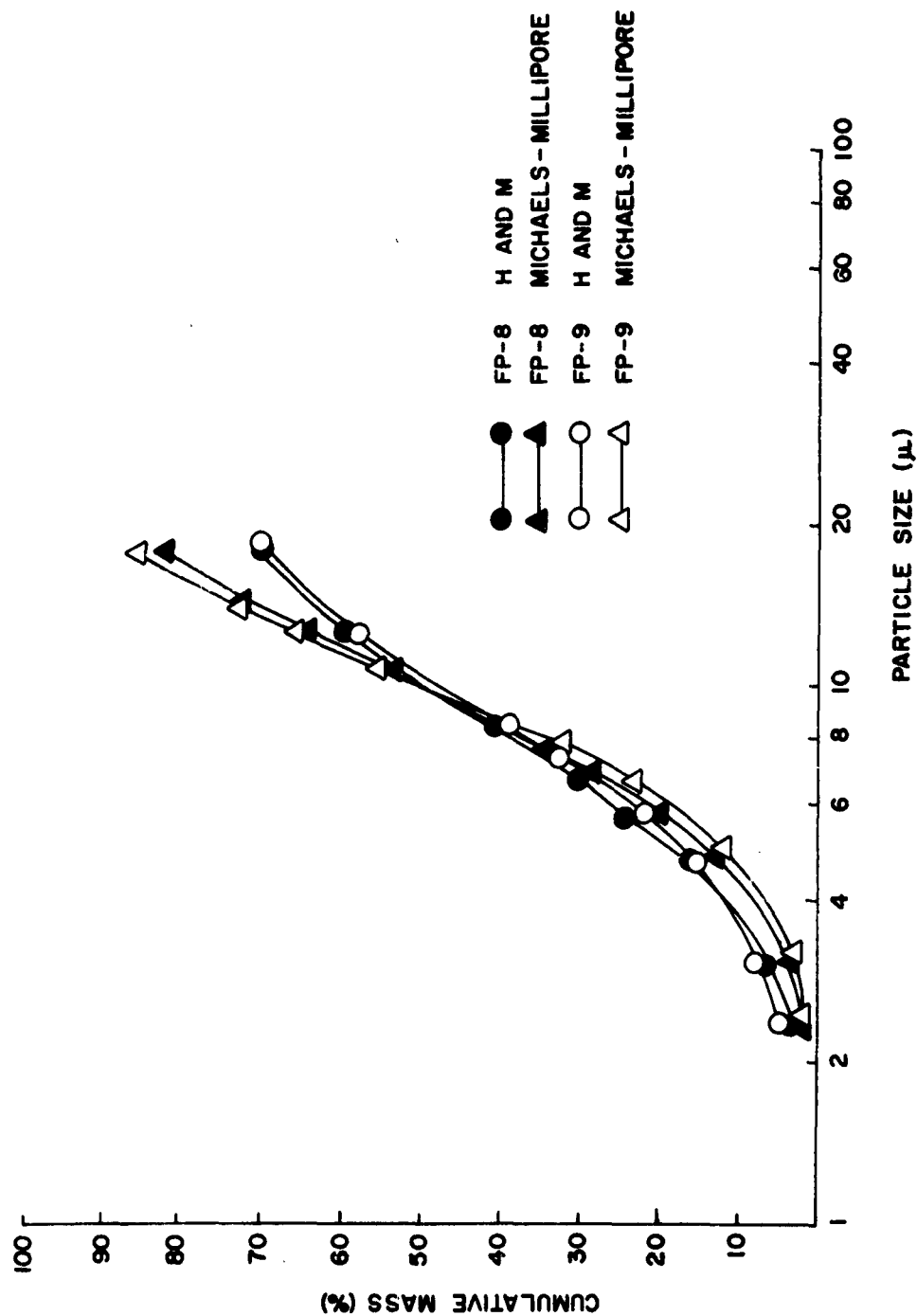


Figure 23. Data Reduction Comparison of two Methods - Stirred Settling,
(1) Harner and Musgrave, and (2) Michaels-Millipore.

The plots are illustrated in Figure 24. No trend is indicated due to the surface coating of the particles. The reproducibility appears to be rather good with only minor variations in individual curves. In contrast, the same transmission data were reduced by the Michaels-Millipore procedure. The curves, shown in Figure 25, exhibit a considerably greater spread particularly in the large particle end of the curves.

The constant hiding factor used in the Harner and Musgrave method is greater than Rose's coefficient for the larger particles. This difference tends to minimize distribution curve perturbations in the larger particle areas in the Harner and Musgrave technique as compared to the Michaels-Millipore method. Also, in normalizing with the Millipore factor, small variations in the filter weights tend to magnify the mass correction in the large particle portion of the curve. However, assuming a representative Millipore factor and accurate light transmission measurements, the perturbations of the curves may be more indicative of the aerosol size distribution. The Harner and Musgrave method on the other hand minimizes some of the perturbations and thus yields curves that are more convenient to compare on a relative basis.

How the results from the photoextinction measurements compare with decay curves obtained with Millipore filter should be noted. Average size distribution curves for Tests FP-1, -2, and -5 comparing the two data reduction techniques for photoextinction and the Millipore filter method are shown in Figure 26. The curves appear to agree in these tests, however, discrepancies have been found in other tests. Generally, it is felt that the major derivation is caused by variations in Millipore data during the early sampling period. This is probably due to inhomogeneity of the cloud since, even with the mild stirring used, it requires time to blend the particle concentration gradients.

A comparison of the photoextinction results with other size distribution methods such as the MSA and micromerograph particle analyzers, has not been included in this report. The handling procedures in sampling and operating this particle sizing equipment would be expected to alter the distribution markedly from the airborne cloud. Therefore these methods would not aid in comparing measurements of the actual aerosol. These techniques are useful in comparing particle sizes and for trends with parameter changes and are not necessarily related to the airborne cloud.

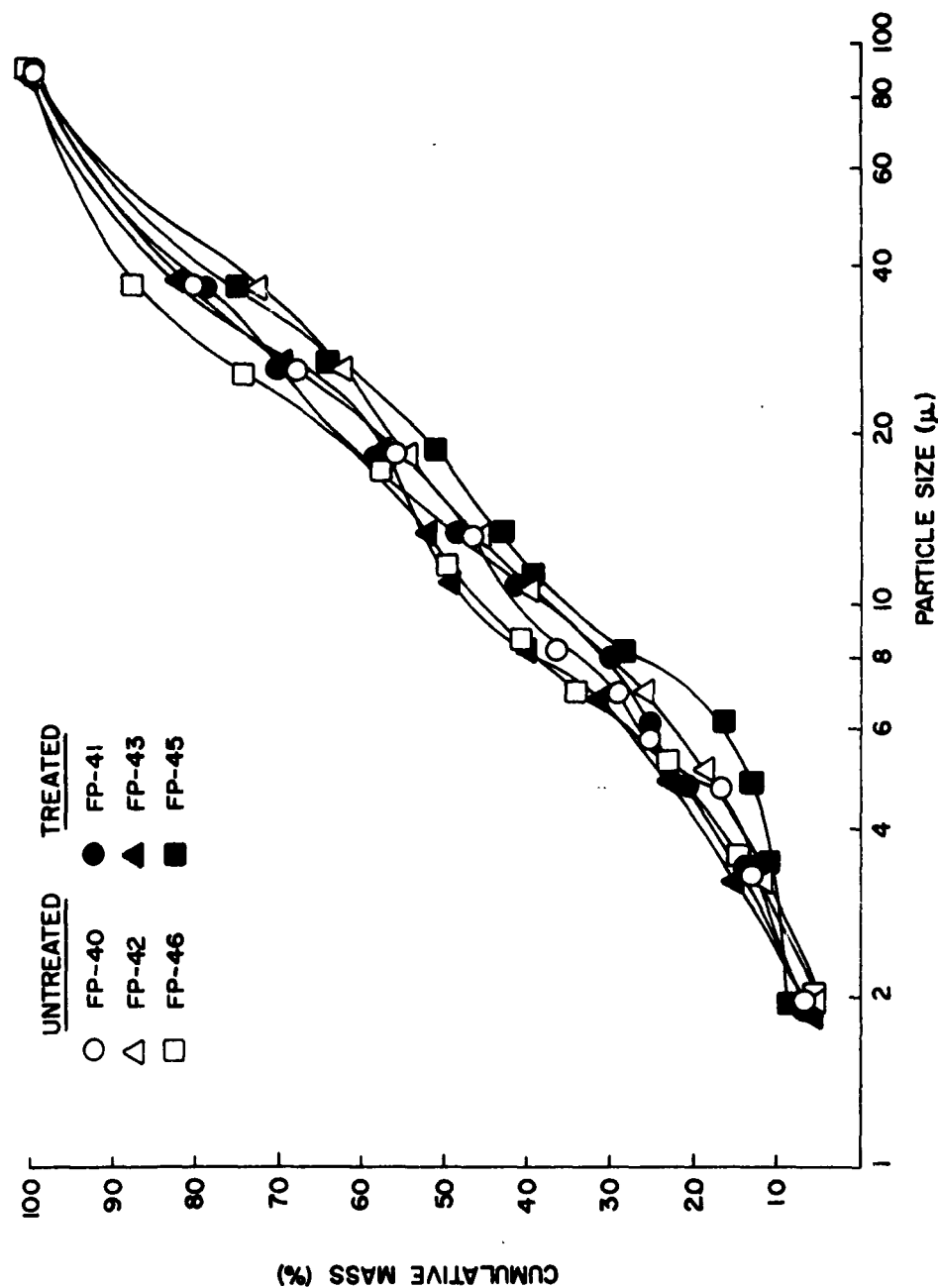


Figure 24. Size-Distribution Curves for Silicone-Coated Silica,
Harner and Musgrave Method.

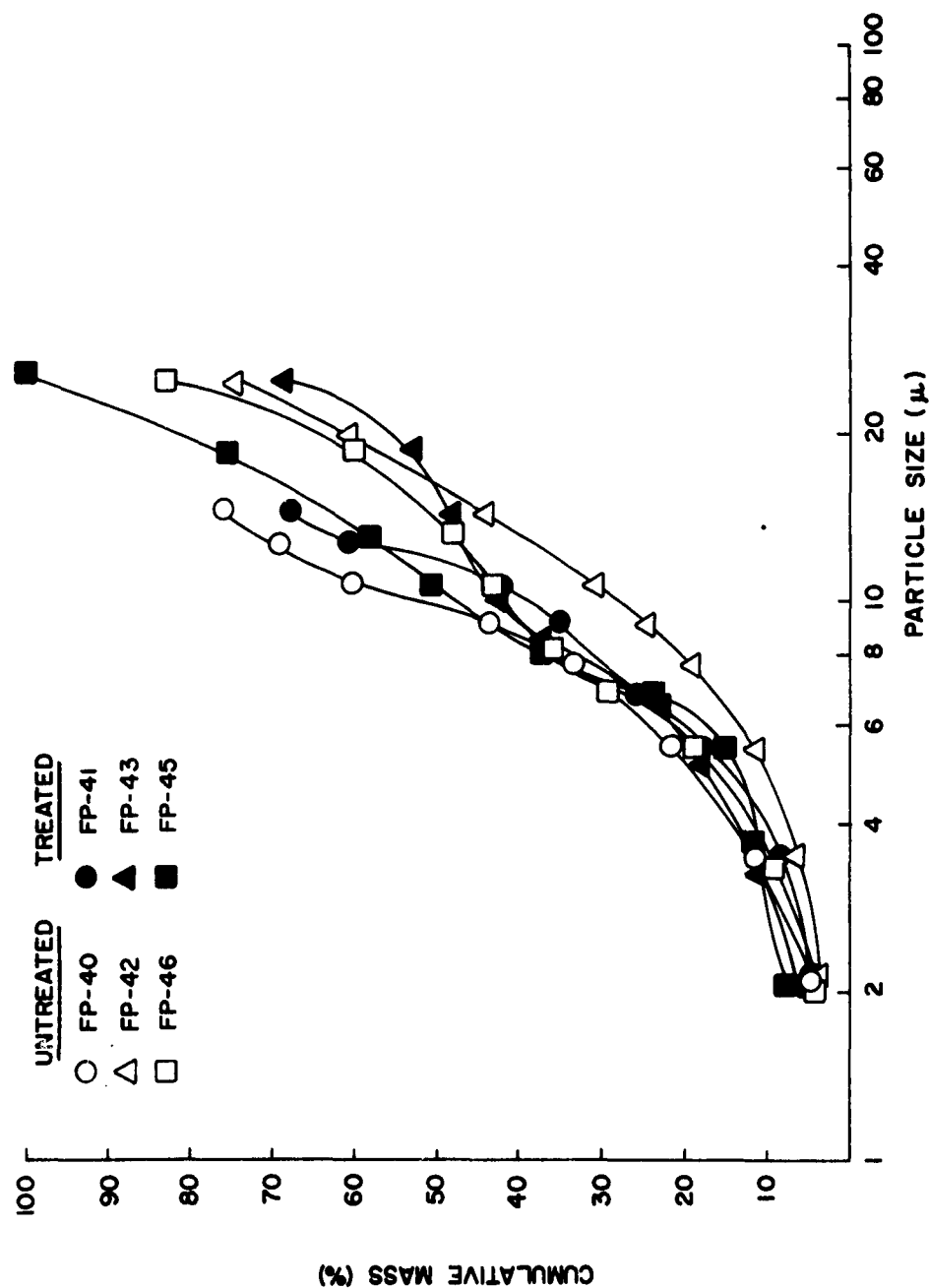


Figure 25. Size-Distribution Curves for Silicone-Coated Silica,
Michaels-Millipore Method.

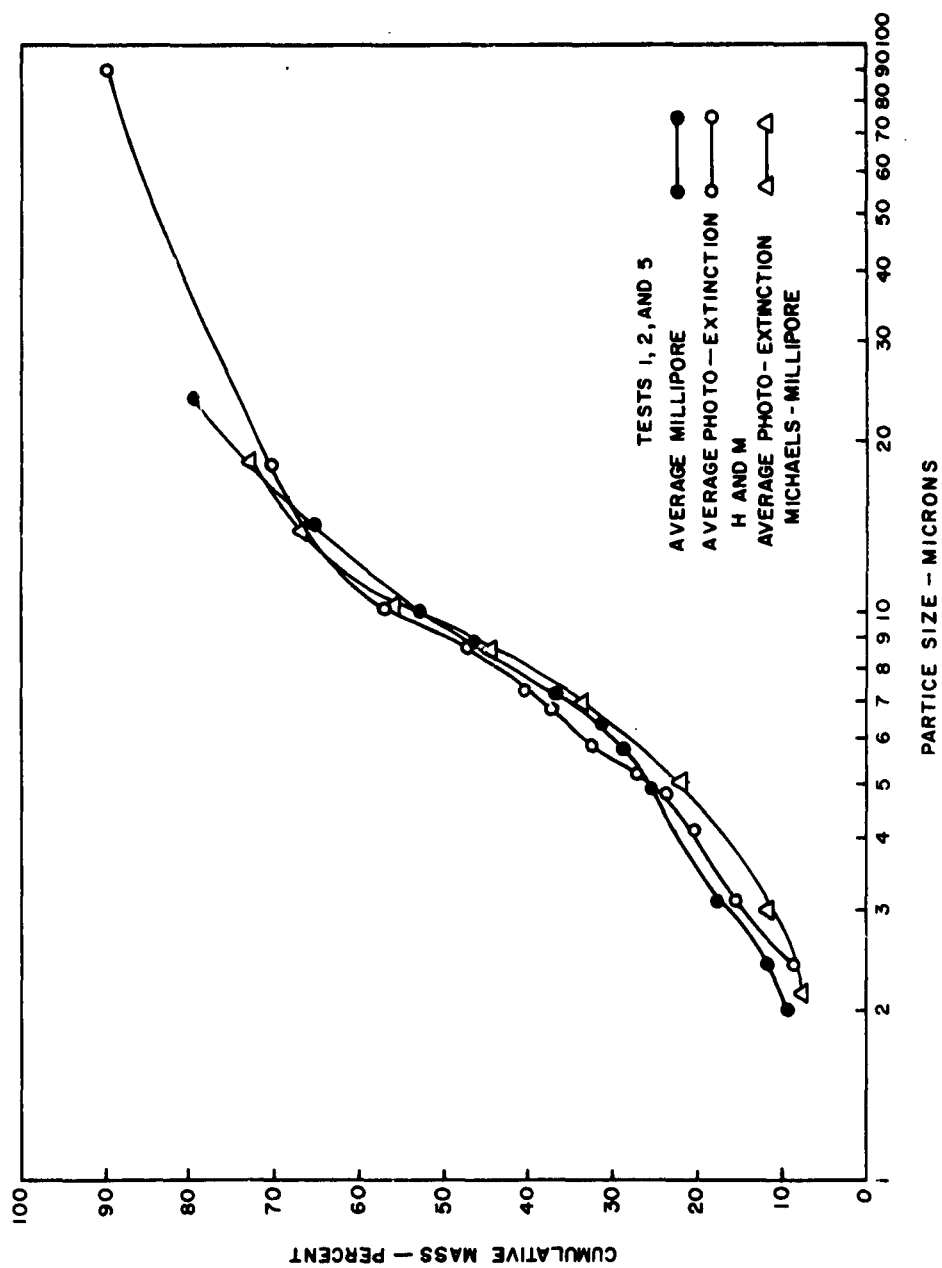


Figure 26. Average Distribution Curves From Photoextinction and Millipore Filters.

7. CONCLUSIONS

It has been demonstrated that the photoextinction method can be a useful tool in studying aerosols in large test chambers. At this stage, the method would appear limited to relative comparisons of particle-size distributions since there are numerous factors such as agglomeration and convection currents which can not completely be accounted for with practical data reduction applications. Also, a particle's conformance with Stokes' and Beer's laws is limited beyond specific size ranges. Experimental conditions affecting homogeneity of the aerosol are of critical importance. Stirred settling produces more consistent results and increases the capacity for measuring the decay of larger particles in the early settling stages. However, from the experimental results it is recognized that the stirring may have a slight, although small, effect on the size distribution results. The procedures, as employed for the reported particle-size determinations, may be improved by further studies to attempt to more closely establish absolute particle sizes. Michaels-Millipore approach should offer the best opportunity to determine absolute particle size; however, the reproducibility by relative methods has given more consistent correlation. In this respect, the Harner-Musgrave approach should be useful in determining the qualitative effects of various parameter changes in experiments. The use of transmission curve extrapolations to estimate (or calculate) maximum particle sizes with the incorporation of Rose's extinction coefficient and the logarithmic function is the most theoretically justifiable technique considered in this study. Calculations made from best-fit polynomial data cause no significant shifts in distribution from extrapolated techniques except in cases where several experimental points are out of line. These perturbations in the curve should be significant, unless inhomogeneities are responsible, and therefore, they should be included in the size distributions calculated. The inhomogeneities should be dealt with through improving the stirring of the chamber or preparing more consistent dissemination devices. Empirical methods for calibrating the photometric system may offer the best possibility for correlating data with absolute particle sizes.

8. RECOMMENDATIONS

The following recommendations are made for continuing the development of the photoextinction particle-size assessment technique:

- a. Improve instrumentation by better collimation of the light beam with a suitable optical system, modify the electrical apparatus to ensure controlled power input, and redesign the photoreceiver and light source housing units to improve mechanics of operation.
- b. Conduct additional calculations on available data, along with new data, to more completely evaluate correlation of data reduction methods. The data presented in this report suggest certain conclusions that should be supported with further results or modifications in calculations. The Michaels-Millipore method for example, should include duplicate or triplicate filter samples to ensure reliable Millipore normalizing factors. This should be compared with the Harner and Musgrave approach applying also the logarithmic function of Beer's law and Rose's extinction coefficients.
- c. Methods for improving homogeneity of the aerosols with controlled stirring should be further studied. Effective height factors in the Stoke's equation should be considered for specific parameters of dissemination devices.
- d. Empirical calibration of the assessment apparatus may be made using standard spherical particles. Nonexplosive dissemination techniques and antielectrostatic coatings may help minimize biases due to agglomeration.
- e. Tests should be conducted with other materials to determine if factors such as refractive index, light scattering, and particle shape impart significant variations in the system used.

REFERENCES

1. Dallavalle, J. M., Micromeritics, Pitman Publishing Corp., New York, N. Y., 1943.
2. Schwyer, H. E., and L. T. Work, "Methods for Determining Particle-Size Distribution," Symposium on New Methods for Particle-Size Determination in the Subsieve Range, Am. Soc. Testing Mats, 1941.
3. Stutz, G. F. A, "The Scattering of Light by Dielectrics of Small Particle Size," Journal, Franklin Institute, Philadelphia, Pa., Vol. 210, 57-85 (1930).
4. Richardson, E. G., "An Optical Method for Mechanical Analysis of Soils," Journal, Agricultural Soc., Vol. 24, 457-468 (1934).
5. Richardson, E. G., "Turbidity Measurements by Optical Means," Proceedings, Physical So. (London), Vol. 55, 48-63 (1943).
6. Skinner, D. G., and A. G. Withers, "Sampling and Analysis of Dust Raised in Suspension in Coal Mines," Transactions, Institution of Mining Engineers (London), Vol. 105, 676-703 (1946).
7. Alexander, J., "Colloid Chemistry," Vol. 1, Chemical Catalogue Co., New York, N. Y. (1926).
8. Rose, H. E., "The Measurement of Particle Size in Very Fine Powders," Chemical Publishing Co., Inc., New York, N. Y. (1954).
9. Skinner, D. G., and S. Boas-Traube, "The Light Extinction Method of Particle-Size Estimation," Symposium on Particle-Size Analysis, Supplement to Transactions, Institution of Chemical Engineers (London) Vol 25, 57-63 (1947).
10. Toman, R. C., et al., "Relation Between Intensity of a Tyndall Beam and Size of a Particle," Journal, Am. Chem. Soc., Vol 41, 575 (1919).
11. Orr, C., Jr., and J. M. Dallavalle, Fine Particle Measurement, The MacMillan Co., New York, N. Y., 1959.

12. Cadle, R. D., Particle-Size Determination, Interscience Publishers, Inc., New York (1955).
13. Irani, R. R., and C. F. Callis, "Particle-Size Measurement, Interpretation, and Application," John Wiley and Sons, Inc., New York (1963).
14. Symposium on Particle-Size Measurement, 61st Annual Meeting, American Society for Testing Materials, ASTM Special Technical Publication No. 234 (1958).
15. Davies, C. N., "The Sedimentation of Small Suspended Particles," Symposium on Particle-Size Analysis, Institution of Chemical Engineers, (London) (1947).
16. Binder, R. C., Fluid Mechanics, Prentice-Hall, Inc., New York, N. Y. (1949).
17. Roller, P. S., "Metal Powder Size Distribution with the Roller Analyzer," Symposium on Testing Metal Powders and Metal Powder Products, Am. Soc. Testing Mats., 54-65 (1952); ASTM STP No. 140.
18. Andreasen, A. H. M., "Validity of Stokes' Laws for Nonspherical Particles," Kolloid-Zeitschrift, Vol. 48, 179 (1929).
19. Boyd, C. K., "The Theory of Sedimentation and Decay of Aerosols," Interim Report BLIR-7, Chemical Corps Biological Laboratories, Camp Detrick, Maryland (July 1952).
20. "Military Problems with Aerosols and Nonpersistent Gases," Summary Technical Report of Division 10, NDRC, Vol. 1, Office of Scientific Research and Development, National Defense Research Committee, Division 10, Washington, D. C. (1946).
21. "Research Study on the Dissemination of Solid and Liquid Agents," Aerojet-General Corporation Quarterly Progress Report 0395-04(05)QP (1963).